Dissertation zur Erlangung des Doktorgrades

der Fakultät für Chemie und Pharmazie

der Ludwig-Maximilians-Universität München

The endosomal adaptor protein LAMTOR2 is essential for invariant natural killer T cell development

Lina Wendeler

aus Oerlinghausen, Deutschland

2022

Erklärung

Diese Dissertation wurde im Sinne von § 7 der Promotionsordnung vom 28. November 2011 von Herrn Prof. Dr. med. Dr. sci. nat. Christoph Klein betreut und von Herrn Prof. Dr. med. Veit Hornung von der Fakultät für Chemie und Pharmazie vertreten.

Eidesstattliche Versicherung

Diese Dissertation wurde eigenständig und ohne unerlaubte Hilfe erarbeitet.

München, 10.11.2022

Lina Wendeler

Dissertation eingereicht am: 30.08.2022

1. Gutachterin / 1. Gutachter: Prof. Dr. med. Veit Hornung
2. Gutachterin / 2. Gutachter: Prof. Dr. med. Dr. sci. nat. Christoph Klein

Mündliche Prüfung am: 27.10.2022

Acknowledgements

During my laboratory research work and thesis writing, I have received a lot of support and I would like to take the opportunity to thank everyone, who has been involved:

I was financially supported by a DFG fellowship through the Graduate School of Quantitative Biosciences Munich (QBM) and subsequently by a Care-for-Rare fellowship, for which I am very grateful.

I gratefully acknowledge my external supervisor Prof. Dr. med. Dr. sci. nat. Christoph Klein, who rendered his valuable time and effort for helpful suggestions and fruitful discussions.

Special thanks go to my project supervisor, Dr. Daniel Kotlarz, who was very generous with his time and knowledge and assisted me in each step to complete this thesis.

I would further like to thank my internal thesis supervisor, Prof. Dr. Veit Hornung, for his great support and valuable guidance throughout my studies.

I would like to acknowledge Dr. Dashtsoodol Nyambayar for kindly providing the 2E10 NKT hybridoma cell line and the NIH Tetramer Core Facility for kindly providing the following reagents: Mouse CD1d-PBS-57-Tetramer-BV421 and Mouse CD1d-unloaded-Tetramer-BV421.

Furthermore, I would like to thank all team members of the AG Klein/Kotlarz for giving me helpful suggestions on this project and for the nice working atmosphere.

Finally, I would like to thank my family and friends, especially Madlin and Caro, for their love and great support.

Zusammenfassung

Invariante natürliche Killer-T-Zellen (iNKT-Zellen) weisen Eigenschaften von konventionellen T- und natürlichen Killerzellen auf und fungieren als Verbindungsstück zwischen der adaptiven und der angeborenen Immunantwort. Die iNKT-Zellentwicklung im Thymus ist sowohl abhängig von der endo-lysosomalen Prozessierung von Glykolipiden in doppelt positiven T-Zellen, als auch von verschiedenen Signalwegen, die das Überleben, die Differenzierung und die Proliferation von iNKT-Zellen vermitteln. In vorangegangenen Studien wurde gezeigt, dass das späte endosomale Adaptorprotein LAMTOR2 eine wichtige Rolle im endo-lysosomalen Trafficking und in der räumlich-zeitlichen Regulation von Signalwegen spielt, jedoch wurde die Funktion von LAMTOR2 während der iNKT-Zellentwicklung bisher noch nicht untersucht.

Um die Rolle von LAMTOR2 in der iNKT-Zellentwicklung zu erforschen, haben wir Mäuse mit einem T-Zell-spezifischen Knockout von *Lamtor2* im frühen doppelt negativen 2/3 T-Zell-Entwicklungsstadium generiert. Unsere Daten zeigen, dass die Deletion von *Lamtor2* schwere Defekte in der frühen iNKT-Zellentwicklung im Thymus verursacht, was zu einer signifikant reduzierten Anzahl an peripheren iNKT-Zellen in der Milz und Leber führt, während die konventionelle T-Zellentwicklung intakt bleibt. Weiterhin konnten wir zeigen, dass LAMTOR2 dabei in zwei wichtige Prozesse während der iNKT-Zellentwicklung involviert ist. Zum einen führt die Deletion von *Lamtor2* zu einer beeinträchtigten Glykolipidpräsentation in doppelt positiven T-Zellen, die für die positive Selektion von iNKT-Zellen wichtig ist. Zum anderen führt das Fehlen von LAMTOR2 zu einer reduzierten Aktivität des mTORC1-Signalweges und vermehrtem Zelltod während des Übergangs vom frühen Entwicklungsstadium ST1 zum Entwicklungsstadium ST2 nach der Positivselektion. Darüber hinaus wiesen *Lamtor2* KO Mäuse eine fehlende Glykolipid-vermittelte Aktivierung peripherer iNKT-Zellen und eine geringere akute Thymusinvolution (ATI) in einem CCL_4-induzierten ATI-Mausmodell auf. Unsere Ergebnisse zeigen somit, dass LAMTOR2 eine wesentliche Rolle bei der Entwicklung und Funktion von iNKT-Zellen spielt.

Summary

Invariant natural killer T cells (iNKT) cells exhibit characteristics of conventional T and natural killer cells and function as a bridge between the adaptive and innate immune response. The development of iNKT cells in the thymus is dependent on the endo-lysosomal processing of glycolipids by double positive T cells and various cell signaling pathways mediating cell survival, differentiation and proliferation of iNKT cells. The late endosomal adaptor protein LAMTOR2 has been shown to play significant roles in endo-lysosomal trafficking and the spatiotemporal regulation of cell signaling pathways, however, the function of LAMTOR2 during iNKT cell development has not been studied yet.

In order to investigate the role of LAMTOR2 during iNKT cell development, we generated mice with a T cell-specific knockout of *Lamtor2* at the early T cell developmental stage double negative 2/3. We show that *Lamtor2* deletion causes severe defects in early iNKT cell development in the thymus, resulting in significantly reduced numbers of peripheral iNKT cells in spleen and liver, while conventional T cell development remains intact. Our data demonstrates that LAMTOR2 is involved in two important processes during iNKT cell development. First, loss of LAMTOR2 causes impaired glycolipid presentation on double positive T cells, which is important for positive selection of iNKT cells. Second, ablation of LAMTOR2 results in reduced mTORC1 signaling and increased cell death during the transition from developmental stage ST1 to developmental stage ST2, subsequently to positive selection. In addition, loss of LAMTOR2 causes unresponsiveness of peripheral iNKT cells to glycolipid-mediated activation and inhibits acute thymic involution (ATI) in a CCL_4-induced ATI mouse model. Thus, our findings show that LAMTOR2 plays an essential role in the development and function of iNKT cells.

Table of Contents

List of Figures

List of Tables

List of Abbreviations

aGC	α-Galactosylceramide
AKT	AKT serine/threonine kinase
AP-2/3	adapter protein-2/3
APCs	antigen presenting cells
ATI	acute thymic involution
BCL10	B-cell lymphoma/leukemia 10
BCR	B cell receptor
BrdU	bromodeoxyuridine
CCl_4	carbon tetracloride
CD	cluster of differentiation
CHS	Chediak-Higashi syndrome
CLB	Cell Lysis Buffer
cMYB	MYB proto-oncogene, transcription factor
cMYC	MYC proto-oncogene, transcription factor
CTL	cytotoxic T lymphocyte
D segment	diversity segment
DAG	diacylglycerol
DCs	dendritic cells
DN	double negative
DOCK1/2	dedicator of cytokinesis 1/2
DP	double positive
Egr1 and 2	early growth response 1 and 2
ELISA	Enzyme-linked Immunosorbent Assay
ER	endoplasmatic reticulum
ERK	mitogen-activated protein kinase 1
ETPs	early thymic progenitor cells
FACS	fluorescence-activated cell sorting
FLT3	Fms related tyrosine kinase 3
FVS	Fixable Viability Stain
FYN	FYN proto-oncogene, Src family tyrosine kinase
GATA3	GATA binding protein 3

List of abbreviations

GS	Griscelli syndrome
h	hours
HC+β_2m	CD1d-β2-microglobulin heterodimers
HIV	human immunodeficiency virus
HPS	Hermannsky-Pudlak syndrome
HRP	Horseradish peroxidase
i.p.	intraperitoneally
IBD	Inflammatory Bowel Disease
IEI	inborn errors of immunity
IFN	interferon
IL	interleukin
iNKT	invariant natural killer T
IP_3	inositol 1,4,5-trisphosphate
iTCR	invariant T cell receptor
ITK	Il-2 inducible T cell kinase
J segment	joining segment
KO	knockout
LAMTOR2	late endosomal/lysosomal adaptor, MAPK and MTOR activator 2
LAT	linker for activation of T cells
LCK	lymphocyte cell-specific protein-tyrosine kinase
LCs	Langerhans cells
LPS	lipopolysaccharide
MFI	mean fluorescence intensity
MHC	major histocompatibility complex
min	minutes
MP1	late endosomal/lysosomal adaptor, MAPK and MTOR activator 3
mTORC1	mammalian target of rapamycin complex 1
NFAT	nuclear factor of activated T cells
NFKB	nuclear factor kappa B
NK	natural killer

List of abbreviations

p70S6K	ribosomal protein S6 kinase beta-1
PBMCs	peripheral blood mononuclear cells
PBS	Phosphate Buffered Saline
PBS-T	PBS-Tween
PCR	polymerase chain reaction
PI3K	phosphatidylinositol-4,5-bisphosphate 3-kinase
PID	primary immunodeficiency
PIP_2	phosphatidylinositol-4,5-bisphosphate
PKCθ	protein kinase θ
PLCγ1	phospholipase Cγ1
PLZF	promyelocytic leukaemia zinc finger
p-p70S6K	phospho-p70S6K
pre-TCRα	*ptrca*
PVDF	polyvinylidene fluoride
qPCR	quantitative real-time PCR
Raptor	*Regulatory associated protein of mtor complex 1*
RasGAP	Ras GTPase-activating protein
RasGRP1	Ras guanyl nucleotide-releasing protein 1
RBC	Red Blood Cell
RORγt	retinoic acid receptor-related orphan receptor γt
RT	room temperature
RUNX1	RUNX family transcription factor 1
SAP	SH2 domain containing 1a
SDS	sodium dodecyl sulfate
sec	seconds
SHIP	SH2 domain–containing inositol phosphatase
SLAMf	signaling lymphocytic activation molecule family
SLP-76	SH2 domain-containing leukocyte protein of 76 kDa
SP	single positive
SPF	Specific-Pathogen-Free
ST0-3	iNKT developmental stage 0-3
STAT3	signal transducer and activator of transcription 3

List of abbreviations

TBET	t-box transcription factor 21
TBS	Tris Buffered Saline
TCF1	transcription factor T cell factor 1
TCF12	transcription factor 12
TCR	T cell receptor
TGFβ1	transforming growth factor beta 1
Th1	T helper type 1
TLR	toll-like receptor
TNF	tumor necrosis factor
UTR	untranslated region
V	Volt
V segment	variable segment
VAV1	Vav guanine nucleotide exchange factor 1
WT	wild type
ZAP-70	zeta chain of T cell receptor associated protein kinase 70

1. Introduction

1.1 The late endosomal/lysosomal adaptor protein LAMTOR2 regulates mTORC1 and ERK signaling in cells of the immune system

The late endosomal/lysosomal adaptor, MAPK and MTOR activator 2 (LAMTOR2, also known as ROBLD3, p14) protein has been first identified in 2001 [4]. It is expressed in various cells of the immune system (e.g., monocytes, macrophages, neutrophils, B cells, T cells, dendritic cells (DCs) and natural killer (NK) cells) and other organs and tissues, such as the nervous system, lung, liver, muscle, intestine, secretory system and reproductive system (based on: ProteomicsDB, MaxQB, MOPED, TISSUES 2 databases [5-8]).

Structure biological and biochemical analyses demonstrated that LAMTOR2 and late endosomal/lysosomal adaptor, MAPK and MTOR activator 3 (MP1) together are required for ERK activation on late endosomes [9,10]. Subsequently, LAMTOR2 has been described as a constitutive component of the pentameric Ragulator complex, which locks mTORC1 to the lysosomal surface upon amino acid signals [11,12]. Later, this complex has been renamed to the “LAMTOR” complex, consisting of the LAMTOR1-5 proteins. Analysis of the crystal structure of the pentameric LAMTOR complex (Fig. 1 [3]) has shown that LAMTOR2 and LAMTOR3 form a heterodimer and they both exhibit two alpha helices, which are important for protein-protein-interactions. A second heterodimer is formed by LAMTOR4 and LAMTOR5, which is surrounded by the adaptor LAMTOR1.

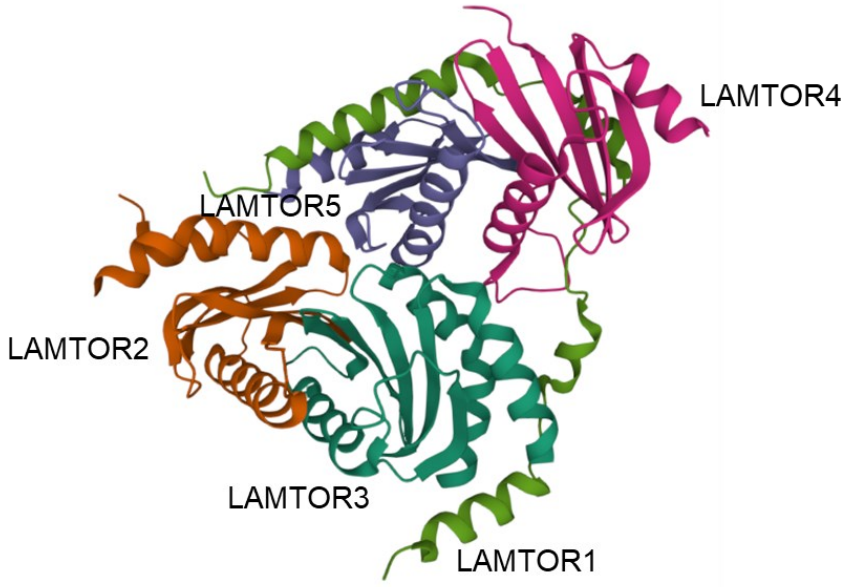

Figure 1: Crystal structure of the pentameric LAMTOR complex, which consists of 5 LAMTOR proteins [1-3]. LAMTOR2 forms a heterodimer together with LAMTOR3. The two alpha helices in LAMTOR2 and LAMTOR3 mediate interactions with other proteins.

LAMTOR2 has been shown to play a significant role in the spatiotemporal regulation of mammalian target of rapamycin complex 1 (mTORC1) and mitogen-activated protein kinase 1 (ERK) signaling pathways at the late endosome (Fig. 2) [4,9-14]. First studies on knockout (KO) mice showed that loss of *Lamtor2* is embryonic lethal and highlighted that LAMTOR2 is essential for cellular proliferation during early embryogenesis and tissue homeostasis in a mouse model with an epidermis-specific deletion of *Lamtor2* [13].

Both ERK and mTORC1 pathways are critically involved in various fundamental processes coordinating protein synthesis, cell growth, proliferation, differentiation, apoptosis, migration, lipid biosynthesis, and autophagy [15-19]. LAMTOR2 plays an important role in regulating these processes in immune cells. For example, LAMTOR2 mediates cell homeostasis via regulation of Fms related tyrosine kinase 3 (FLT3)-dependent mTORC1 signaling in DCs, leading to a myeloproliferative expansion of the DC compartment [20]. *Lamtor2*-deletion in Langerhans cells (LCs) reduces transforming growth factor beta 1 (TGF-β1) sensitivity resulting in impaired homeostasis and immunological function of LCs [21,22]. Furthermore,

conditional deletion of LAMTOR2 in monocytes, mature macrophages and granulocytes resulted in an increased susceptibility to Lipopolysaccharide (LPS) in a sepsis mouse model (unpublished data). Finally, functional studies of LAMTOR2-deficient B cells showed that activation of the B cell receptor (BCR) resulted in impaired BCR internalization, intracellular signaling, and proliferation [23]. In summary, these studies have documented that the spatiotemporal endosomal regulation of signal transduction pathways by LAMTOR2 controls several aspects of innate and adaptive immune responses.

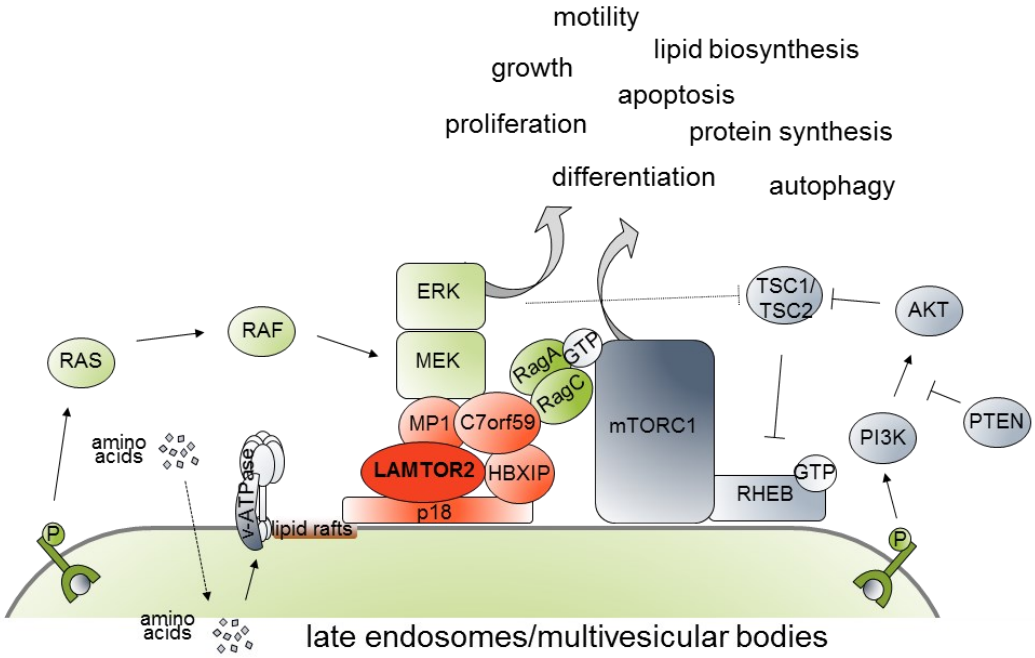

Figure 2: LAMTOR2 regulates mTORC1 and ERK signaling spatiotemporally on late endosomes/multivesicular bodies in cells of the immune system (figure adapted from Daniel Kotlarz). LAMTOR2 functions as a key regulator of various cellular processes, like motility, lipid biosynthesis, cell growth, apoptosis, proliferation, protein synthesis, differentiation, and autophagy [15-19].

1.2 Human LAMTOR2 deficiency causes a primary immunodeficiency syndrome

Primary Immunodeficiencies (PID; more recently subsumed under the general term “inborn errors of immunity”, IEI) are a large and heterogeneous group of diseases that affect the development and/or function of the innate and adaptive

immune system [24]. Patients with PID are more susceptible to common and opportunistic infections and may predispose individuals to allergy, inflammation, autoimmune disorders, and malignancy [25]. Although the individual diseases are rare, all PIDs combined appear in around 1% of the overall population [26]. To date, 482 different genetic entities have been reported [27]. PID can be classified into 10 different categories: immunodeficiencies affecting cellular and humoral immunity, combined immunodeficiencies with syndromic features, predominantly antibody deficiencies, diseases of immune dysregulation, congenital defects of phagocytes, defects in intrinsic and innate immunity, autoinflammatory diseases, complement deficiencies, bone marrow failure, and phenocopies of inborn errors of immunity [28].

In contrast to secondary Immunodeficiencies, which develop from other diseases (e.g., human immunodeficiency virus (HIV)) or immunosuppressive medications, PIDs are caused by inherited or acquired defects in genes which play important roles in the development or function of the human immune system [28]. An individual genetic mutation in a patient, inherited by the Mendelian rules, can cause a monogenic disease [28]. Advances in NGS have improved diagnosis in patients suspected for monogenic disease and have been implemented in clinical routine [29].

Using linkage studies, transcriptomic profiling and candidate gene sequencing, our laboratory has previously identified a novel PID syndrome in a white Mennonite index family, caused by a homozygous point mutation in the 3’ untranslated region (UTR) of the late endosomal/lysosomal adaptor, MAPK and MTOR activator 2 gene (*Lamtor2*, also known as *Robld3*, *p14*) [30]. LAMTOR2-deficient patients presented with severe congenital neutropenia, growth failure, partial albinism, and B and cytotoxic T lymphocyte (CTL) deficiencies. The 3’ UTR mutation in LAMTOR2-deficient patients has been shown to generate a 5' splice site which is recognized by the spliceosome, leading to suppression of *LAMTOR2* poly(A)-site 3' end processing [31]. Cell biological studies of our laboratory in LAMTOR2-deficient patient cells showed a perturbed subcellular distribution of late endosomes and suggested an important role of LAMTOR2 in the regulation of endosomal trafficking in

immune cells and biosynthesis of lysosomal-related organelles (e.g. azurophilic and lytic granules, and melanosomes) in neutrophils, CTLs and melanocytes [30,32].

LAMTOR2 deficiency is grouped into a constellation of PIDs, affecting multiple organelles related to lysosomes, such as Griscelli syndrome (GS), Hermannsky-Pudlak syndrome (HPS), and Chediak-Higashi syndrome (CHS) [32] (Fig. 3). Affected proteins associated with these diseases are regulators of intracellular protein trafficking and organelle movement. For example, HPS type 2 is characterized by the deficiency of the adapter protein-3 (AP-3) complex, which leads to aberrant trafficking of translysosomal proteins [33-35]. Individuals with HPS type 2 present with clinical manifestations similar to LAMTOR2 deficiency, e.g., congenital neutropenia, CTL deficiency, and partial albinism. Abnormal azurophilic granules of neutrophils, defective lytic granules of CTLs, aberrant melanosomes of melanocytes have been proposed as potential causes accounting for these phenotypes. Furthermore, individuals with HPS type 2 lack invariant natural killer T (iNKT) cells, caused by an impaired cluster of differentiation 1d (CD1d)-mediated glycolipid processing and presentation of $CD4^+CD8^+$ double positive (DP) thymocytes towards iNKT cells [33,36]. However, the role of LAMTOR2-mediated endosomal trafficking in iNKT cell development and function remains elusive. In view of limited access to patient material, we were not able to study the development and function of iNKT cells in human LAMTOR2-deficiency. Therefore, we generated mice with a T cell-specific KO of *Lamtor2* to analyze the function of LAMTOR2 in iNKT cells.

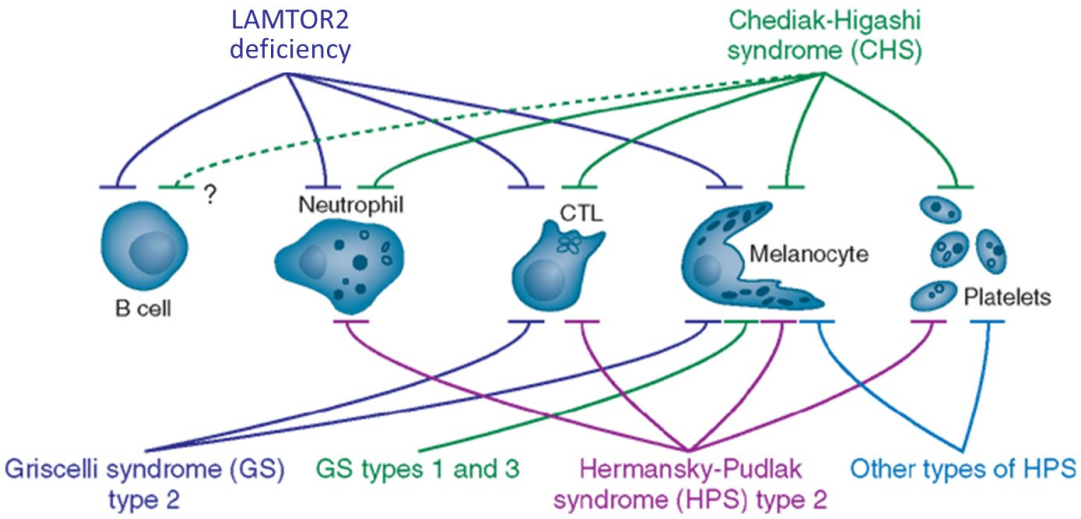

Figure 3: Overview of PIDs affecting multiple organelles related to lysosomes (modified from [32]). Patients with LAMTOR2 deficiency, CHS, GS type 2, GS type 1 and 3, HPS and other types of HPS show overlapping manifestations in multiple organelles related to lysosomal, e.g., azurophilic granules of neutrophils, lytic granules of CTLs, melanosomes of melanocytes and dense granules of platelets.

1.3 Characterization of invariant natural killer T (iNKT) cells

Invariant natural killer T cells (iNKT) cells are a subtype of T lymphocytes, which share characteristics of conventional T cells and of natural killer (NK) cells, and thereby connect innate and adaptive immune responses [37]. They play an important role in various pro- and anti-inflammatory immunological processes, like immune responses against pathogens and cancer, but are involved in the development of autoimmune and inflammatory conditions as well [38].

iNKT cells express a semi-invariant T cell receptor (TCR), which contains a single segment of Vα and Jα DNA (Vα14-Jα18 in mice, Vα24-Jα18 in humans) combined with one of three Vβ segments (Vβ8, Vβ2, or Vβ7 in mice, Vβ11 in humans) [39]. Murine iNKT cell subsets express CD4 ($CD4^+CD8^-$ subset) or neither CD4 nor CD8 ($CD4^-CD8^-$ double negative (DN) subset), whereas a subset of CD8 positive cells ($CD4^-CD8^+$ subset) can be detected in human [38]. Furthermore, iNKT cells carry other T cell markers, which are characteristic for activated or memory phenotypes, such as CD25, CD44, CD69 and CD122 [40]. Notably, iNKT cells also express NK cell lineage

markers, including NK1.1 in mice or CD161 in humans, as well as CD16 and CD56.

1.3.1 Murine iNKT cell development differs from conventional T cell development

Upon transition of early thymic progenitor cells (ETPs) from the bone marrow to the cortex of the thymus, they undergo T lineage specification and develop through $CD4^-CD8^-$ DN stages 1-4, which can be distinguished by the differential expression of CD44 and CD25 (DN1: $CD4^-CD8^-CD44^+CD25^-$, DN2: $CD4^-CD8^-CD44^+CD25^+$, DN3: $CD4^-CD8^-CD44^-CD25^+$ and DN4: $CD4^-CD8^-CD44^-CD25^-$) [41,42]. Next, developing T cells upregulate CD4 and CD8 and become $CD4^+CD8^+$ DP T precursor cells (Fig. 4). Whereas conventional T cells develop into $CD4^+$ and $CD8^+$ single positive (SP) T cells, iNKT cell development deviates off from conventional T cell development [43-45]. Developing iNKT cells subsequently pass three mayor steps: (i) the rearrangement of an invariant TCR (iTCR) for lineage commitment of iNKT cells, (ii) the positive selection of iNKT cells, and (iii) an expansion and differentiation phase of positively selected iNKT cells, as described in 1.3.2-4.

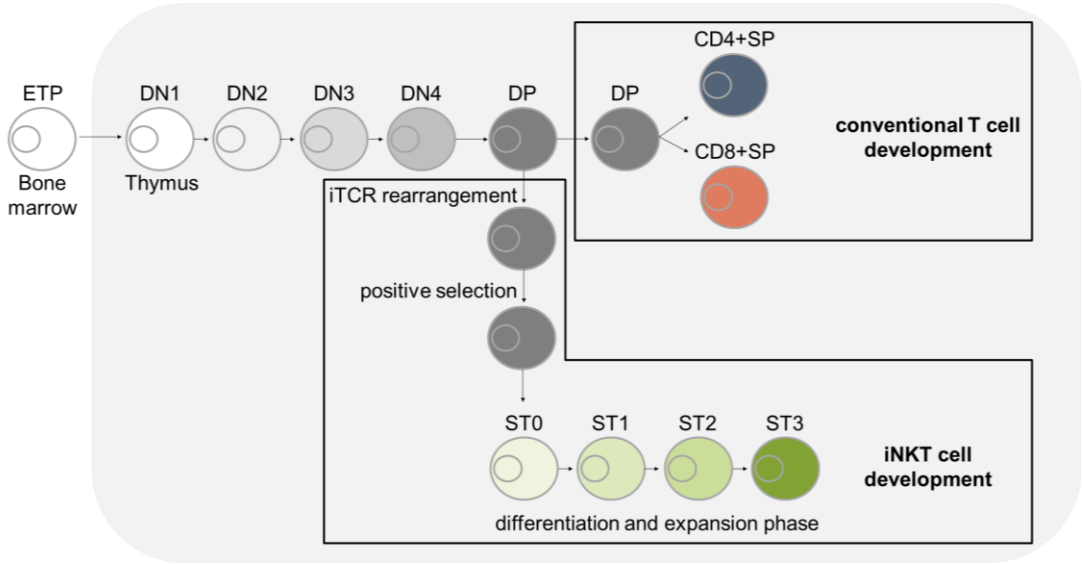

Figure 4: Schematic overview of conventional T and iNKT cell development. Modified from [46]. Upon entry into the thymus, early thymic progenitor (ETP) cells develop through stages DN1 to DN4. Upregulation of surface markers CD4 and CD8

results in DP T cells. Whereas conventional T cells propagate to $CD4^+$ SP and $CD8^+$ SP T cells, iNKT cell development branches off at the DP stage. The three major following steps of iNKT cell development are the iTCR rearrangement, positive selection and a subsequent differentiation and expansion phase.

1.3.2 iTCR rearrangement of iNKT cells

TCR rearrangement is a process of somatic recombination of the variable (V), diversity (D), and joining (J) TCR gene segments (V(D)J recombination) [47]. This process appears at the late DP precursor stage in a stochastical manner, resulting in a highly diverse repertoire of TCRs in conventional $CD4^+$ and $CD8^+$ T cells. In contrast, lineage commitment of iNKT cells occurs by rearranging a specific proximal Va segment with a specific distal Jα segment (Vα14-Jα18), combined with one of three specific Vβ segments (Vβ8, Vβ2, or Vβ7) [48]. These rearrangements result in a semi-invariant Vα14-Jα18/Vβ8, Vβ2, or Vβ7 iTCR, which is a unique feature of iNKT cells (Fig. 5). In contrast to conventional T cells that recognize peptides presented on MHC molecules, the iTCR recognizes glycolipid antigens presented on CD1d molecules [49]. Therefore, iNKT cells can be uniquely identified using a tetramer, consisting of four CD1d molecules, bound to a glycolipid antigen that specifically binds to the iTCR (PBS57/CD1d tetramer, [50]).

Mouse models that fail to generate Va-Ja rearrangements usually exhibit a reduced lifetime of precursor DP thymocytes, resulting in reduced iNKT cells numbers. Examples for mice with this phenotype exhibit a deficiency of transcription factor 12 (TCF12), retinoic acid receptor-related orphan receptor γt (RORγt), RUNX family transcription factor 1 (RUNX1), transcription factor T cell factor 1 (TCF1), and MYB proto-oncogene, transcription factor (cMYB) [39,51-53].

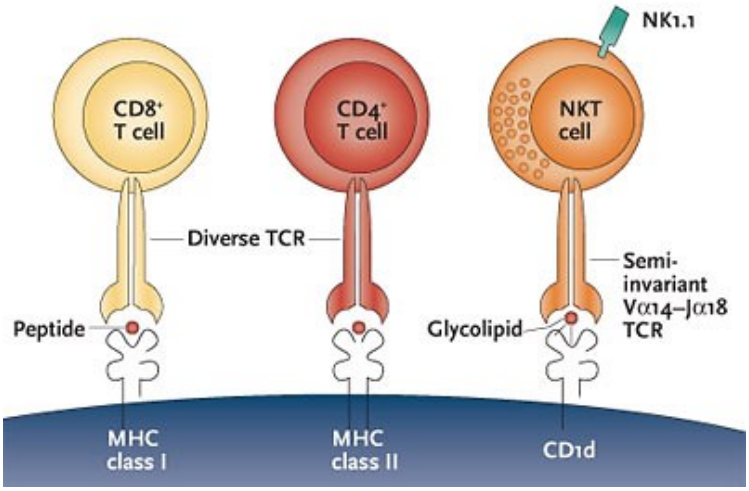

Figure 5: T cell receptors of conventional CD4+ and CD8+ T cells and iNKT cells (modified from [54]). Conventional T cells possess a highly diverse repertoire of T cell receptors, which recognize peptide antigens presented on major histocompatibility complex (MHC) molecules. In contrast, iNKT cells express a semi-invariant TCR consisting of Vα14-Jα18/Vβ8, Vβ2, or Vβ7 rearrangements. This iTCR specifically interacts with glycolipid antigens presented on CD1d molecules.

1.3.3 Positive selection of iNKT cells

Once TCR rearrangement has occurred, iNKT cells undergo positive selection, a process to ensure that a newly rearranged TCR is able to recognize MHC or CD1d complexes [55]. While cortical thymic epithelial cells present peptide antigens to conventional T cells, positive selection of iNKT cells is mediated by glycolipid-loaded CD1d on DP thymocytes of hematopoietic origin [56]. The synthesis of CD1d molecules is very similar to MHC class I molecules [49,57]. Newly synthesized CD1d-β2-microglobulin heterodimers (HC+β_2m), carrying a lipid cargo, travel through the secretory pathway to the cell surface [58]. However, in contrast to MHC class I molecules, the processing and loading of glycolipid antigens onto CD1d molecules require trafficking though the endo-lysosomal system, because glycolytic enzymes and lipases need an acidic pH to process the glycolipid antigens and prepare them for presentation on the cell surface (Fig. 6). Importantly, mice with a deletion of CD1d, or only the deletion of the cytoplasmic tail of CD1d, lack iNKT cells, demonstrating that the CD1d tail motif is critically for glycolipid antigen presentation [57,59,60]. Furthermore, the adapter proteins AP-2 and AP-3 have been shown to be

essential for CD1d-mediated antigen processing though the endo-lysosomal pathway [33,36,61].

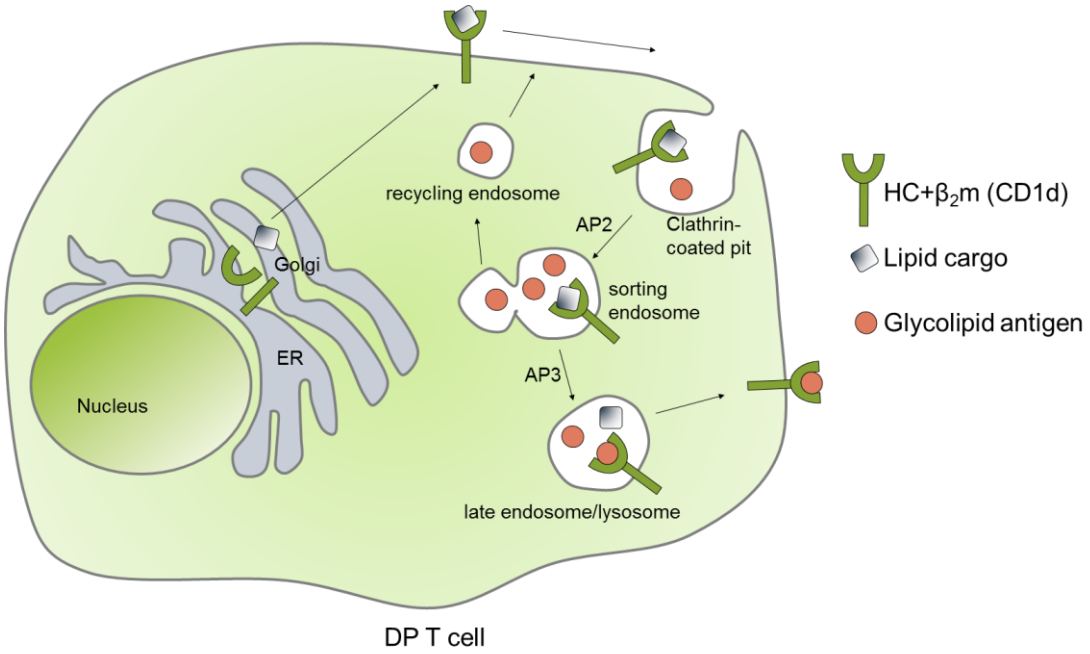

Figure 6: CD1d-mediated processing and glycolipid antigen presentation. Modified from [49]. The HC and β_2m chains assemble in the endoplasmatic reticulum (ER) to form the CD1d molecule, which is loaded with a lipid cargo in the Golgi and then traffics through the secretory pathway towards the cell surface. Upon clathrin-mediated endocytosis, CD1d travels through the endo-lysosomal pathway, facilitated by the adaptor proteins AP-2 and AP-3. The acidic pH in the late endosome/lysosome leads to processing of lipid antigens, which are loaded onto CD1d. Next, the glycolipid-loaded CD1d molecule travels back to the cell surface in order to present the glycolipid for positive selection of iNKT cells.

Once glycolipids have been processed and are presented on the cell surface of DP T cells, the CD1d-glycolipid complex can interact with an iTCR from developing DP NKT cells, leading to positive selection (Fig. 7). Mice with deletion of components of the TCR signaling pathway show impaired positive selection of iNKT cells, e.g. mice with deficiency of the CD3ζ chain, lymphocyte cell-specific protein-tyrosine kinase (LCK), zeta chain of T cell receptor associated protein kinase 70 (ZAP-70), SH2 domain-containing leukocyte protein of 76 kDa (SLP-76), Il-2 inducible T cell kinase (ITK), linker for activation of T cells (LAT) and Vav guanine nucleotide exchange factor 1 (VAV1). [62-69]. In addition, co-stimulatory signals of the signaling lymphocytic activation molecule family (SLAMf) surface receptors, which are expressed on

NKT cell precursors as well as cortical DP thymocytes, have also been shown to be crucial for positive selection [70]. Activation of the SLAMf receptor leads to recruitment of the adaptor molecule SH2 domain containing 1a (SAP), which in turn activates the Src family tyrosine kinase FYN [71]. Mice with deficiency of SLAMf receptors, SAP or FYN show severely diminished iNKT cell development [70,71].

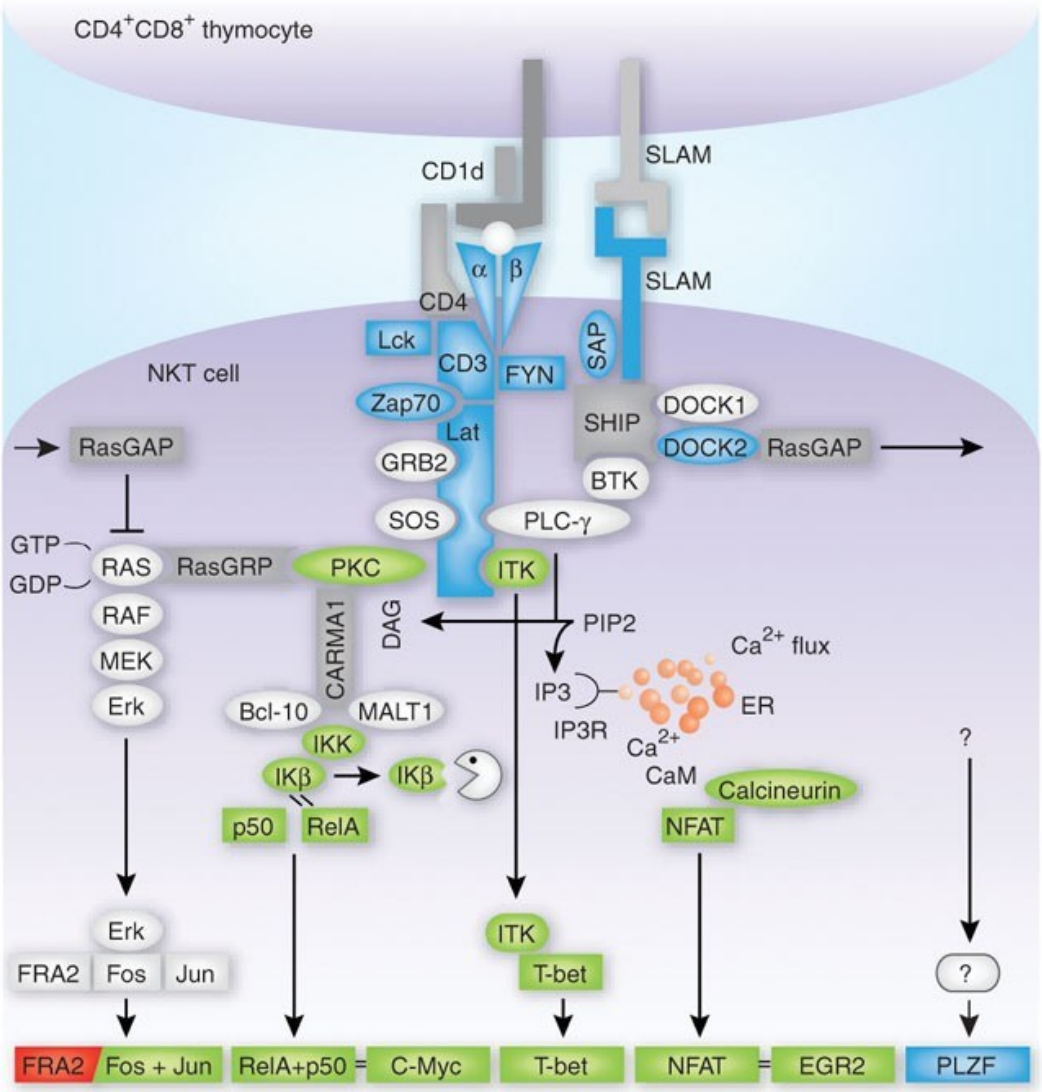

Figure 7: Overview of positive selection of iNKT cells [72]. $CD4^+CD8^+$ DP thymocytes present glycolipids on CD1d and send co-stimulatory signals from SLAMf surface receptors towards the iNKT cell. A successfully positively selected iNKT cell activates ERK, nuclear factor kappa B (NFKB), ITK and inositol 1,4,5-trisphosphate (IP3) signaling pathways in order to activate a transcriptional program for subsequent differentiation and maturation.

1.3.4 Differentiation, proliferation and survival of iNKT cell precursors after positive selection

Upon positive selection in the thymus, iNKT cells proceed through developmental stages 0–3: stage 0 ($CD24^+CD44^-NK1.1^-$), stage 1 ($CD24^-CD44^-NK1.1^-$), stage 2 ($CD24^-CD44^+NK1.1^-$) and stage 3 ($CD24^-CD44^+NK1.1^+$). However, the final maturation to the $NK1.1^+$ stage can also occur in the periphery (Fig. 8). While immature $NK1.1^-$ NKT cells progress through a post-selection proliferation phase, mature $NK1.1^+$ NKT cells in the thymus are non-cycling cells [62]. Based on the surface expression of CD44 and NK1.1 as well as the transcription factor expression of t-box transcription factor 21 (TBET), GATA binding protein 3 (GATA3) and RORyt, NKT cells can also be divided into functional NKT1, NKT2 and NKT17 subsets [73,74].

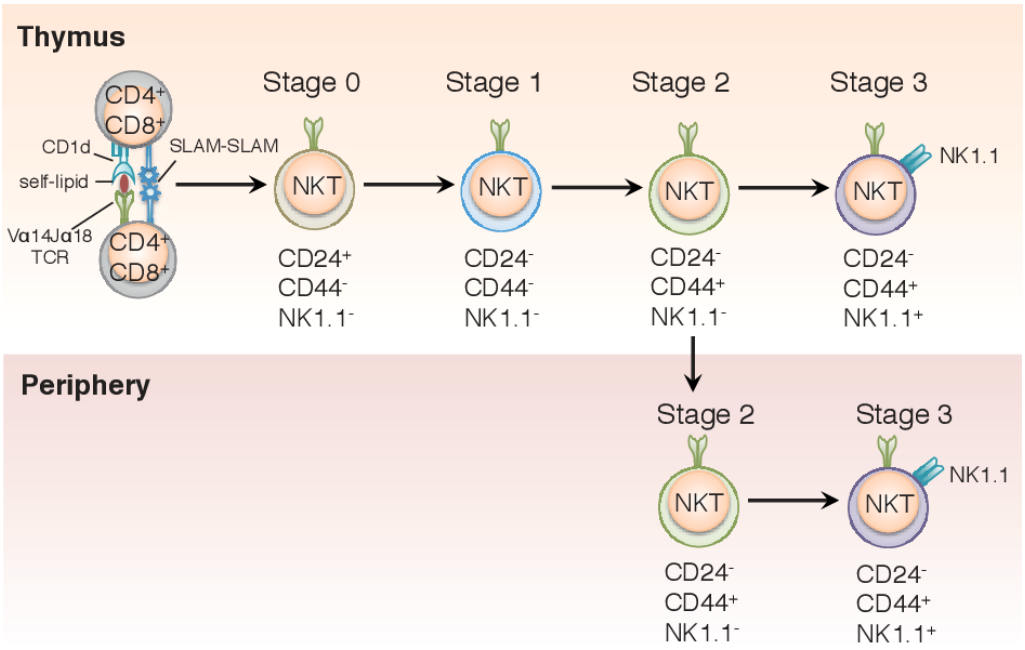

Figure 8: Stages of NKT cell development [75]. Upon positive selection, developing thymic iNKT cells pass through stage 0 (CD24+CD44-NK1.1-), stage 1 (CD24-CD44-NK1.1-), stage 2 (CD24-CD44+NK1.1-) and stage 3 (CD24-CD44+NK1.1+) in order to become fully mature iNKT cells. The maturation step from Stage 2 to Stage 3 can occour in the thymus as well as in the peripheral organs.

Differentiation, proliferation and survival of NKT cells upon positive selection are tightly regulated processes involving various signaling pathways and transcription factors (Fig. 7).

iTCR stimulation during positive selection activates proximal tyrosine kinases LCK and ZAP70 to phosphorylate phospholipase Cγ1 (PLCγ1), which in turn catalyzes the reaction from phosphatidylinositol-4,5-bisphosphate (PIP_2) to diacylglycerol (DAG) and inositol-1,4,5-triphosphate (IP_3), which act as second messengers [76-78]. DAG triggers activation of the Ras guanyl nucleotide-releasing protein 1 (RasGRP1)-Ras-Erk1/2 pathway, which is crucial for iNKT cell development [79]. Activation of the ERK pathway leads to the activation of the phosphatidylinositol-4,5-bisphosphate 3-kinase(PI3K)/AKT serine/-threonine kinase (Akt) pathways, which triggers mTORC1 and mTORC2 activation [78,80]. Mice with T cell–restricted deletion of *Regulatory associated protein of mtor complex 1* (*Raptor*), a member of the mTORC1 complex, show impaired iNKT cells but normal conventional T cell development [81]. Furthermore, DAG activates the NF-κB pathway via protein kinase θ (PKCθ) and the B-cell lymphoma/leukemia 10 (BCL10) adaptor protein [82,83]. The NFκB pathway is required for the transition of $NK1.1^-$ precursors to mature $NK1.1^+$ NKT cells. Correspondingly, mice with a KO of *p50/ NFκB1* or *p52/ NFκB2* exhibit strongly reduced frequencies of NKT cells [84]. Both, ERK and NF-κB signaling pathways trigger the expression of the transcription factor MYC proto-oncogene, transcription factor (cMYC), which is required for the proliferation phase of iNKT cells after positive selection. cMYC-deficient mice show a developmental block of iNKT cells between stage 0 and stage 1 [85].

The second messenger IP_3 stimulates calcium release from the endoplasmic reticulum (ER), which leads to dephosphorylation and nuclear translocation of the transcription factor nuclear factor of activated T cells (NFAT) [86]. NFAT activates expression of early growth response 1 and 2 (Egr1 and 2), which in turn activate promyelocytic leukemia zinc finger (PLZF) expression, a key regulator of early NKT cell development [87,88]. Mice with KO of *Plzf* and *Egr2* mice exhibit a strong reduction of mature thymic iNKT cells but show normal conventional T cell development [62,89].

Another signaling cascade downstream of the iTCR is ITK activation, which triggers phosphorylation of TBET. Murine TBET deficiency causes a developmental block of iNKT cell development at stage 2 [90].

Signals from SLAMf lead to the activation of SAP and FynT, which phosphorylate the SH2 domain–containing inositol phosphatase (SHIP), dedicator of cytokinesis 1/2 (DOCK1/2), and Ras GTPase-activating protein (RasGAP), which in turn negatively regulates ERK signaling [70,91]. Furthermore, the SLAM-SAP–FynT pathway cross talks with the iTCR signaling pathway to activate the NF-κB via PKCθ and BCL10 [92].

1.3.5 iNKT cells in health and disease

Although iNKT cells are a rare type of immune cells, comprising only 0.01-1.2% of peripheral blood mononuclear cells (PBMCs) in humans [93], they are more frequently found in liver, spleen, thymus, and bone marrow. Highest frequencies of iNKT cells are found in the liver (around 30 % of intrahepatic lymphocytes are iNKT cells [94]).

iNKT cells can be activated by two general mechanisms [38]. First, iNKT cells can be indirectly activated through the interaction of toll-like receptor (TLR) agonists with TLRs on antigen presenting cells (APCs), leading to cytokine production and activation of iNKT cells. Second, APCs endocytose, process, and present endogenous or exogenous glycolipids on CD1d molecules to iNKT cells, leading to a direct activation. The most prominent glycolipid antigen is α-Galactosylceramide (aGC), which was isolated from the marine sponge *Agelas mauritianus*, and has extensively been used to study iNKT cell biology [95].

As iNKT cells show characteristics of an activated or memory phenotype, they have a great capacity to rapidly produce various cytokines upon TCR activation [38]. They produce T helper type 1 (Th1) cytokines (e.g. interferon (IFN)γ, and tumor necrosis factor (TNF)), Th2 cytokines (e.g. interleukin (IL)-4, and IL-13) or Th17 cytokines (e.g. IL-17) [73].

iNKT cells play an important role in the initiation and regulation of immune responses against bacteria, viruses, fungi, protozoa and parasites [38,96]. Upon infection, microbial glycolipid antigens can be loaded onto CD1d

molecules of APCs, leading to rapid production of cytokines, which subsequently recruit and activate immune cells of the innate and adaptive immune system. iNKT-deficient mice (*Cd1d*$^{-/-}$ or *Jα18*$^{-/-}$ mice) have been shown to exhibit an impaired host defense against Borrelia Burgdorferi, *Novosphingobium* and *Ehrlichia* genera, *Chlamydia muridarum,* encephalomyocarditis virus, herpes simplex virus type 1 and 2 (HSV-1, HSV-2) [97-102]. In humans, iNKT cells show effector functions against Candida albicans, HIV, hepatitis C virus (HCV) and influenza A virus (IAV) and immune-modulating functions during Aspergillus fumigatus infections [103-107].

Furthermore, iNKT cells have been shown to contribute to anti-tumor immunity [108,109]. They play a mostly protective role as they produce IFN-γ to activate NK and CD8^{+} T cells, which in turn can lyse tumor cells. aGC administration has been shown to boost anti-tumor responses in mouse studies [110-114]. In addition, iNKT cells stimulated DCs to produce IL-12, which contributed to anti-tumor effects [108,115,116]. Human studies provided additional evidence that iNKT cells contribute to anti-tumor immunity [117-120]. These studies have led to a number of clinical trials to treat cancer patients with aGC, however no significant benefit from aGC therapy was observed [121-123].

In addition, iNKT cells can promote several autoimmune and inflammatory conditions [38]. In mice, iNKT cells have been shown to contribute to the pathogenesis of arthritis, allergic airway inflammation, atherosclerosis, contact hypersensitivity, colitis, ischemia-reperfusion injury, sickle cell disease and sepsis syndrome [38,124-131]. In humans, iNKT cells were shown to be increased in peripheral blood from children with severe therapy-resistant asthma and in the sputum of asthmatic patients [132,133]. Furthermore, pro-inflammatory iNKT cells were increased in the lamina propria of inflammatory bowel disease (IBD) patients [134].

Besides their pro-inflammatory functions, iNKT cells also have immunomodulatory properties, because they protect mice from multiple sclerosis, graft-versus-host disease, type 1 diabetes and systemic lupus erythematosus [135-139]. Reduced frequencies of iNKT cells in the peripheral blood of patients with multiple sclerosis, type 1 diabetes, and systemic lupus

erythematosus patients were observed, suggesting a similar function for iNKT cells in humans. [140-143].

In the pathogenesis of liver disease, iNKT cells were shown to play both protective as well as pathogenic roles in a mouse model of carbon tetracloride (CCl4)-induced liver injury [144]. However, most recent studies propose a stronger pro-inflammatory role for iNKT cells in liver injury [145,146]. In humans, the role of iNKT cells in the development of liver fibrosis are still unclear, as both pro- and anti-fibrotic functions have been proposed [147-149].

In summary, extensive research showed that iNKT cells are involved in many immunological processes, e.g., immune response against pathogens, anti-tumor immunity, autoimmunity and liver fibrosis [38]. As iNKT cells are a rare cell population of the immune system, research is challenging and has been done mostly in mice. More studies are needed to clearly define the role of iNKT cells in health and disease.

2. Aim of the PhD thesis

In this study, we generated mice with a T cell-specific KO of *Lamtor2* at the early T cell developmental stage DN2/DN3. We observed significantly reduced proportions of iNKT cells in KO versus wild type (WT) mice. Therefore, we hypothesize that LAMTOR2 plays a critical role in the development and function of iNKT cells. The overall goal of this thesis was to study the role of LAMTOR2 in the regulation of iNKT cell development. This knowledge will provide critical insights into molecular mechanisms of LAMTOR2 deficiency in immune cells.

The specific aims of the PhD thesis are:

a. To analyze the function of LAMTOR2 in CD1d-mediated glycolipid antigen-processing in DP T cells during positive selection of iNKT cells.

b. To determine the role of LAMTOR2 in the regulation of cell signaling pathways subsequently to positive selection of iNKT cells.

c. To investigate if LAMTOR2 plays an important role in peripheral iNKT cell activation and in the development of a murine acute thymic involution (ATI) mouse model.

3. Materials and methods

3.1 Materials

All used chemicals, buffers, consumables, machines, tools, regents and kits are listed in Table 1-5.

Table 1: List of chemicals.

Chemical	**Company**	**Order number**
5-Bromo-2'-deoxyuridine (5-BrdU)	Jena Bioscience	N-DN-1136-5G
Agarose Basic	Applichem	A8963
Ammonium Chloride	Sigma Aldrich	A9434-500G
Ammonium Persulfate	Serva	13375.02
Bromphenol Blue	Roth	A512.1
Carbon Tetrachloride	Sigma-Aldrich	289166-100ML
Ethanol absolut ≥99.5%, TechniSolv®, rein	VWR	83813-440
Ethidium bromide	Applichem	A1152,0010
Glycerol ROTIPURAN® ≥99.5 %, p.a.	Roth	3783.1
Glycin PUFFERAN® ≥99 %, p.a.	Roth	3908.3
Milk Powder Blotting Grade	Carl Roth	T145.3
Ortho-Phosphoric Acid (H_3PO_4) 85%	Roth	6366.1
Roti-Stock 20% SDS	Carl Roth	1057.1
Sodium Chloride	Roth	9265.2
Sodium Dodecylsulfate	Roth	0183.1
Sucrose	Sigma Aldrich	S0389-500G
TEMED	Carl Roth	2367.3
TRIS, 5 kg	Carl Roth	5429.2
Tween ® 20	Applichem	142312.1611
α-Galactosylceramide	hellobio	HB3751

β-Mercaptoethanol	Sigma Aldrich	M6250-100ml

Table 2: List of buffers.

Buffer	**Ingredients**
1 L 10x Running Buffer	144.1 g Glycine 30.3 g Tris 10 g SDS H_2O up to 1 L
1 L 10x Transfer Buffer	144.1 g Glycine 30.3 g Tris 10% Ethanol H_2O up to 1 L
1 L PBS-T	1 L of 1x PBS 0.5 ml Tween20
1 L Red Blood Cell (RBC) Lysis Buffer	8.3 g Ammonium Chloride 100 ml 0.1M Tris-HCL Adjust pH to 7.5 with HCL H_2O up to 1 L
1 L TBS	6.05 g Tris 8.76 g NaCl Adjust pH to 7.5 with HCL H_2O up to 1 L
1 ml 1x Cell Lysis Buffer (CLB)	100 µl 10x Cell lysis buffer (Cell signaling) 10 µl PMSF 60 µl PIC 830 µl H_2O
100 ml Lämmli Buffer	10 ml of 1.5 M Tris (pH6.8) 6 ml 20% SDS 30 ml Glycerol 1.8 g Bromphenol Blue 4% Mercaptoethanol H_2O up to 100 ml

Table 3: List of consumables.

Consumable	Company	Order number
25G Needle	BD Microlance	305760
8 tubes PCR 0,2 ml Multiply µStripPro	Sarstedt	72.991.002
96-WELL FAST THERMAL CYCLING PLATES	Thermo Fischer Scientific	3436907
Amersham Hybond P 0.45 PVDF	GE lifesciences	10600023
B Braun™ 04616057V Omnifix 5 ml Syringe	B Braun	4616057V
Falcon® 70 µm Cell Strainer, White	Corning	352350
FG, OPTICAL ADHESIVE COVERS	Thermo Fischer Scientific	4311971
Filter Blue Cap FACS tubes	BD	352235
Sarstedt Inc MICROTUBES 1.5 ML/1000	Sarstedt	72.706.400
Serologische Pipette 10ml	Sarstedt	86.1254.025
Serologische Pipette 25ml	Sarstedt	86.1685.020
Serologische Pipette 2ml	Sarstedt	86.1252.001
Serologische Pipette 5ml	Sarstedt	86.1253.001
TC dish 100	Sarstedt	83.3902
TC-6 Well Plates	Sarstedt	83.3920.300
TC-96 Well Plates, Flat bottom	Sarstedt	83.3924.005
TC-96 Well Plates, round bottom	Sarstedt	83.3925.500
tips SafeSeal SurPhob Spitzen,10 µl, extra lang	Biozym	VT0200
tips SafeSeal SurPhob Spitzen,100 µl	Biozym	VT0230
tips SafeSeal SurPhob Spitzen,1250 µl	Biozym	VT0270
Tube 15ml	Sarstedt	62.554.502

Tube 50ml	Sarstedt	62.547.254

Table 4: List of machines and tools.

Machine/Tool	**Company**
96 Universal Gradient PEQSTAR PCR machine	Peqlab
ABI StepOnePlus	Applied Biosystems
BD FACS Aria™III	BD
BD LSR Fortessa	BD
Centrifuge 5424 R	Eppendorf
Centrifuge 5810 R	Eppendorf
ChemiDocTM XRS+	BioRAD
Eppendorf Research Plus Pipettes (10, 100, 1000)	Eppendorf
Forceps 91197-00	FST
Heracell 204i Incubator	Thermo Fischer
Mini-PROTEAN® Vertical Electrophoresis Cell, 4-gel, for 0.75 mm thick handcast gels, #1658000FC	BioRAD
NanoDrop 2000	Thermo Scientific
Orbital Shaker Polymax 1040	Heidolph
Pipetus®	Hirschmann
Scissors 91460-11	FST
Synergy H1 Hybrid Reader	BioTek
Thermomixer comfort	Eppendorf

Table 5: List of reagents and kits.

Reagent/Kit	**Company**	**Order number**
eBioscience™ TMB Solution (1X)	Invitrogen	00-4201-56
APC BrDU Kit	BD	552598
BD Cytofix/Cytoperm™ solution	BD	554722

BD Fixable Viability Stain 700	BD	564997
BlueRay Prestained Protein Marker	Jena Bioscience	PS-103
Cell Lysis Buffer (10x)	Cell Signaling	9803S
DirectPCR Lysis Reagent Tail	Peqlab	31-102-T
DPBS, no calcium, no magnesium	Thermo Fischer Scientific	14190144
Gibco™ Fetal Bovine Serum	Gibco	10500064
Gibco™ Trypan Blue Solution, 0.4%	Gibco	15250061
HEPES (1M) 100ml	Gibco	15630056
High-Capacity cDNA Reverse Transcription Kit	Thermo Fischer Scientific	4368813
Mid Range DNA Ladder	Jena Bioscience	M-203L
Mouse CD1d-PBS-57-Tetramer-BV421	NIH Tetramer Core Facility	
Mouse CD1d-unloaded-Tetramer-BV421	NIH Tetramer Core Facility	
Mouse IFN-gamma DouSet ELISA	R&D Systems	DY-485-05
Oligo(dT)18 Primer	Thermo Fischer Scientific	S0132
OneTaq® Quick-Load® 2X Master Mix with Standard Buffer	NEB	M0486L
Penicillin-Streptomycin (5,000 U/mL)	Thermo Fischer Scientific	15070063
PIC Protease Inhibitor Cocktail	Sigma	P8340
PMSF (Protease Inhibitor)	Alpha Diagnostics	PMSF16-S-50
Powrup SYBR Mastermix	Thermo Fischer Scientific	A25778
Proteinase K	Peqlab	04-1070
Restore™ Western Blot Stripping Buffer	Thermo Fischer Scientific	21063
RiboLock RNase Inhibitor	Thermo Fischer Scientific	E00382

RNeasy Plus Mini Kit (250)	Qiagen	74136
ROTI®Quant, 500 ml, 2000 Assays (Küvetten)	Carl Roth	K015.1
ROTIPHORESE®Gel 30 (37,5:1), 1	Carl Roth	3029.1
RPMI 1640 Medium, GlutaMAX™ Supplement	Thermo Fischer Scientific	61870036
Sodium Pyruvate (100 mM)	Thermo Fischer Scientific	11360070
SuperSignal West Dura Extendet Duration Substrate	Thermo Fischer Scientific	34076

3.2 Mouse strain and housing conditions

To study the role of LAMTOR2 in iNKT cell development *pTa-Cre*$^{ki/wt}$ mice (Ptcra$^{tm1(icre)Hjf}$; C57BL/6J background, generated by Prof. Dr. Hans Jörg Fehling, Ph. D., provided by EMMA Mouse Repository, Dr. Susan Marschall) and *Lamtor2*$^{flox/flox}$ mice ([13], C57BL/6J background, provided by Prof. Dr. Lukas Alfons Huber, M.D.) were crossed. *pTa-Cre*$^{ki/wt}$-*Lamtor2*$^{flox/flox}$ mice exhibit a conditional deletion of *Lamtor2* in very early T cell developmental stages (DN2/DN3) in the thymus.

Mouse studies were carried out at the Specific-Pathogen-Free (SPF) animal facility of the LMU Munich according to the "*Deutsches Tierschutzgesetz"*, the Directive 2010/63/EU, and the European Convention for the Protection of Vertebrate Animals used for Experimental and Other Scientific Purposes (ETS no. 123). Animal experiments were analyzed according to international standards such as the ARRIVE guidelines. The mouse studies have been approved by the *Regierung von Oberbayern* on November 28th, 2018.

3.3 Genotyping PCRs

Prior to each experiment mice were genotyped for detection of the *Cre* recombinase and *loxP*-flanked *Lamtor2* [13]. Primer sequences are listed in Table 6.

Table 6: List of genotyping primers.

Primer	Sequence
Cre forward	5'-CCTGGGATGGGAGTGGGACCTG-3'
Cre reverse KI	5'-GATCCAGCACCAGAAGCAAGTGCCTA-3'
Cre reverse WT	5'-GTGAGAGCCAAATAGGGAGGCAAGA-3'
loxP Lamtor2 for [13]	5'-GGTGACTACAACTCCCAGGCG-3'
loxP Lamtor2 rev [13]	5'-TGTTGGCTTGGCTTAGCACC-3'

For genotyping, mouse tails were lysed in 200 µl DirectPCR Lysis Reagent Tail buffer supplemented with 0.2 mg/ml Proteinase K and incubated for 3 – 16 h at 900 rpm and 56 °C. For the inactivation of Proteinase K, samples were heated for 50 minutes (min) at 85 °C. After centrifugation at 10,000 g for 30 seconds (sec), DNA containing supernatants were transferred to a new tube and stored at -20 °C. The reaction mixes for each sample were assembled according to Table 7. The polymerase chain reaction (PCR) programs for the *Cre* PCR and *LoxP Lamtor2* PCR are listed in Table 8 and Table 9, respectively.

Table 7: Reaction mix for genotyping PCRs

Reagent	µl per sample
One*Taq*® Quick-Load® 2X Master Mix	10
Template DNA	1
Primer (each)	1
H_2O	add to 20
Total volume	**20**

Table 8: PCR program for *Cre* PCR.

Step	Temperature	Time	Cycles
1	94 °C	2'00''	
2	94 °C	20''	35 cycles
3	60 °C	30''	
4	72 °C	45''	

5	72 °C	5’00’’	
6	4 °C	Hold	

Table 9: PCR program for *LoxP Lamtor2* PCR.

Step	Temperature	Time	Cycles
1	95 °C	5’00’’	
2	95 °C	30’’	30 cycles
3	58 °C	30’’	
4	72 °C	45’’	
5	72 °C	5’00’’	
6	4 °C	Hold	

To detect the PCR products, a 2% agarose gel containing ethidium bromide (1:10000) in 1x Tris Buffered Saline (TBS) was prepared. Mid Range DNA Ladder (6 µl) and samples were loaded into the gel slots and the gelelectrophoresis was conducted at 120 Volt (V) for 40 min. The gel was imaged using a BioRAD-ChemiDoc^{TM} XRS^{+}.

3.4 Western Blot analysis

To confirm the deletion of LAMTOR2 in the KO mice on protein level, thymocytes and cells from the lymph nodes (LN) were harvested and span down at 350 g, 5 min, 4 °C. The cell pellet was resuspended in 30 µl 1x Cell Lysis Buffer (CLB) and incubated for 40 min on ice. After centrifugation (20 min, max. speed, 4 °C) the supernatant was transferred into a new tube and either directly used for Western blot analysis or frozen at -80 °C.

To analyze the protein quantity, 200 µl Bradford Reagent (1:5 diluted with H_2O) and 1 µl protein sample were mixed in a 96-well plate. After incubation for 10 min at room temperature (RT), the absorption at 595 nm was measured using a Synergy H1 Hybrid Reader.

For preparation of the sodium dodecyl sulfate (SDS)-gel, spacer plates and short plates were clamped together. The reaction mixes for the preparation of SDS-gels are listed in Table 10.

Table 10: Reaction mixes for SDS-Gel preparation.

15% separating gel (10 ml)	**6% stacking gel (4 ml)**
2.4 ml H_2O	2.7 ml H_2O
5 ml acrylamide (30%)	0.8 ml acrylamide (30%)
2.5 ml 1.5 M tris (pH 8.8)	0.5 ml 1 M tris (pH 6.8)
50 µl SDS (20%)	20 µl SDS (20%)
100 µl APS (10%)	40 µl APS (10%)
10 µl TEMED	4 µl TEMED

The separating gel was prepared first and poured between the plates, with leaving enough room for the stacking gel. After polymerization for 20 min, the stacking gel was prepared, poured between the plates and next, the clamp was inserted. The stacking gel polymerized for 20 min and the clamp was removed carefully.

The gel was assembled into the electrophoresis chamber. 6 µl of Lämmli buffer were added to 24 µl of diluted protein samples (20 µg protein/sample) and the samples were incubated for 10 min at 95 °C. 1x running buffer was filled into the gel chamber. 6 µl of protein marker and samples were loaded into the gel slots. The gel electrophoresis was conducted at 80 V for 15 min, followed by ~1.5 h at 125 V. The Western blot sandwich with ethanol-activated polyvinylidene fluoride (PVDF) membrane was assembled and placed into the tank filled with 1x transfer buffer. The transfer ran for 50 min at 400 mA at 4 °C.

The membrane was blocked with 5% milk powder diluted in 1x Phosphate Buffered Saline (PBS) for 2 hours (h). Next, the membrane was incubated with primary antibodies (Table 11) diluted in 5 % milk/PBS on the orbital shaker at 4 °C over night. After 12 h of incubation, the membrane was washed three times with PBS-Tween (PBS-T) for 5-10 min, followed by incubation with Horseradish peroxidase (HRP)-conjugated secondary antibody (diluted in 5% milk/PBS) for 1 h at RT. Prior to chemiluminescence detection, the membrane was washed for 3 x 5-10 min with PBS-T. Next, the membrane was incubated for 2 min with 1 ml Super Signal West Dura Extended Duration Substrate (500

µl of solution A and B each) and then the chemiluminescence was detected using a BioRAD-ChemiDoc™ XRS+. Prior to incubation with the next primary antibody, the membrane was stripped with 8 ml of Stripping buffer for 15 min and washed for 3 x 5 min with PBS-T.

Table 11: List of Western Blot antibodies.

Antibody	Concentration	Company	Order number
Anti-rabbit IgG, HRP-linked Antibody	1:3000	Cell Signaling	#7074
LAMTOR2/ROBLD3 (D7C10) Rabbit mAb	1:1000	Cell Signaling	#8145
β-Actin Antibody (C4)	1:3000	Santa Cruz Biotechnology	sc-47778

3.5 RNA isolation

To detect mRNA expression levels, mRNA was isolated using the RNeasy Plus Mini Kit. Frozen cell pellets were resuspended in 350 µl RLT plus buffer, supplemented with 3.5 µl β-Mercaptoethanol. The next steps were performed according to the manufacturer's instructions (Qiagen). In the final step, RNA was eluted in 16 µl nuclease-free H_2O. RNA concentration was measured using a NanoDrop and RNA was stored at -80 °C.

3.6 cDNA synthesis

Up to 2 µg RNA were used for cDNA synthesis (High-Capacity cDNA Reverse Transcription Kit) in a total reaction volume of 20 µl. The reaction mix per sample was set up in a PCR tube (shown in Table 12). The PCR program for cDNA synthesis is displayed in Table 13. cDNA samples were stored at -20 °C.

Table 12: Reaction mix per sample for cDNA synthesis.

Component	Volume (µl)
Template (RNA)	10
10x RT buffer	2
25x dNTP Mix (100mM)	0.8
10× RT Random Primers	1
Oligo(dT)18 Primer	1
MultiScribe™ Reverse Transcriptase	1
Ribolock	1
Nuclease-free H2O	3.2
Total per reaction	**20**

Table 13: PCR program for cDNA synthesis.

	Step1	Step2	Step3	Step4
Temerature (°C)	25	37	85	4
Time (min)	10	120	5	∞

3.7 Quantitative real-time PCR

To detect mRNA expression levels, quantitative real-time PCR (qPCR) analysis was performed using the Powrup SYBR Mastermix. Each qPCR was run in duplicates. The qPCR was assembled in a 96-Well Fast Thermal Cycling Plate using the components listed in Table 14. qPCR primers are displayed in Table 15.

Table 14: qPCR reaction mix per sample.

Component	Volume (µl)
cDNA (≥2.5 ng/µl)	2.5
SYBR	5
Fw primer	1.25
Rv primer	1.25

Table 15: List of qPCR primers.

Primer	Sequence
Lamtor2 forward	5'-TCTGGGCCGCGTATGATAGG-3'
Lamtor2 reverse	5'-CACGCTGTTATGATGCTGCTACTT-3'
Rps9 forward	5'-CTGGACGAGGGCAAGATGAAGC-3'
Rps9 forward	5'-TGACGTTGGCGGATGAGCACA-3'
Va14-Ja18 forward [150]	5'-TCTAGAATTCTAAGCACAGCAC-3'
Va14-Ja18 reverse [150]	5'-CAATCAGCTGAGTCCCAGCT-3'

The plate was covered with a FG,Optical Adhesive Cover and span down shortly. The qPCR was run on the ABI StepOnePlus instrument using the PCR program summarized in Table 16.

Table 16: qPCR program.

Step	Temperature	Time	Cycles
1	50 °C	2'	
2	95 °C	10'	
3	95 °C	15''	41 cycles
4	60 °C	1'	
5	60 °C - 95 °C	+ 0.3 °C 15''	ramp up

The C_t values were normalized to the housekeeping gene (*Rps9*), then the relative expression levels were calculated. Data are presented as fold induction compared to control samples.

3.8 Flow cytometry

To analyze iNKT and T cell populations by flow cytometry, mice were sacrificed by cervical dislocation and thymus, spleen, and liver were collected and processed to single cell suspensions using 70 µm cell strainers. Splenocytes and hepatocytes were lysed with 1 ml Red Blood Cell (RBC) Lysis Buffer at RT for 5 min and washed with 10 ml 2% FBS in PBS. Up to 1 x 10^7 cells in a total volume of 100 µl were stained with antibodies or tetramer for 30 min at 4 °C. The fluorescence-activated cell sorting (FACS) antibodies are listet in

Table 17, the tetramer is listed in Table 5. Next, cells were washed and resuspended in 300 µl 2% FBS/PBS. Cell populations were analyzed on a BD LSR Fortessa and analysis was carried out using FlowJo Single Cell Analysis Software v10.

For Phosflow analysis, cells were washed with 1 ml 2 % FBS in PBS after surface antibody/tetramer staining and then fixed with 100 µl BD Cytofix/Cytoperm for 30 min at 4 °C. Next, cells were washed twice with 400 µl 1 x BD Perm/Wash (1:10 diluted with H_2O), followed by intracellular staining with Phospho-p70 S6 Kinase Rabbit mAb (Table 17) in a total volume of 100 µl 1x BD Perm/Wash for 60 min at RT. Cells were washed again with 400 µl 1 x BD Perm/Wash and then stained with Goat anti-Rabbit IgG Secondary Antibody - Alexa Fluor 568 (Table 17) in a total volume of 100 µl 1x BD Perm/Wash for 15 min at RT. Finally, cells were washed with 400 µl 1 x BD Perm/Wash, then washed with 1 ml 2 % FBS/PBS, and resuspended 300 µl 2% FBS/PBS prior to FACS analysis.

Table 17: List of FACS antibodies.

Antibody	**Clone**	**Working Concentration**	**Company**	**Order number**
Alexa Fluor® 488 anti-mouse TCR β chain Antibody	H57-597	1:100	BioLegend	109215
APC anti-mouse CD4 Antibody	GK1.5	1:100	BioLegend	100412
Brilliant Violet 510™ anti-mouse CD24 Antibody	M1/69	1:200	BioLegend	101831
Brilliant Violet 650™ anti-mouse/human CD44 Antibody	IM7	1:200	BioLegend	103049
CD45R (B220) Monoclonal Antibody	RA3-6B2	1:100	eBioscience	47-0452-82

Antibody	Clone	Working Concentration	Company	Order number
(RA3-6B2), APC-eFluor 780				
FITC anti-mouse CD1d (CD1.1, Ly-38) Antibody	1B1	1:100	BioLegend	123507
FITC anti-mouse CD3 Antibody	17A2	1:100	BioLegend	100204
Goat anti-Rabbit IgG (H+L) Highly Cross-Adsorbed Secondary Antibody, Alexa Fluor 568	Polyclonal	1:800	Invitrogen	A11036
Pacific Blue™ anti-mouse CD45 Antibody	30-F11	1:100	BioLegend	103126
PE anti-mouse CD19 Antibody	6D5	1:100	Biolegend	115508
PE anti-mouse CD8a Antibody	53-6.7	1:200	BioLegend	100708
PE/Cyanine7 anti-mouse NK-1.1 Antibody	PK136	1:100	BioLegend	108714
PE/Cyanine7 anti-mouse α-GalCer:CD1d complex Antibody	L363	1:100	BioLegend	140516
PerCP/Cyanine5.5 anti-mouse CD25 Antibody	3C7	1:50	BioLegend	101912

Antibody	Clone	Working Concentration	Company	Order number
Phospho-p70 S6 Kinase (Thr389) (108D2) Rabbit mAb	108D2	1:100	Cell Signaling	9234P

3.9 Cell sorting

Thymocytes/splenocytes were resuspended in 500 ul 2% FCS/PBS. Up to 5 x 10^7 cells were stained with CD4-APC (1:100) and CD8-PE (1:100) or B220-APC-AF780 (1:100) and CD19-PE (1:100) for 30 min, 4 °C (Table 17). Next, cells were washed and resuspended in 1 ml 2% FBS/PBS. DP T cells ($CD4^+CD8^+$) and B cells ($B220^+CD19^+$) were sorted on a BD FACS Aria^{TM}III. Sorted cells were span down (350 g, 4 °C) and cultured for activation of 2E10 hybridoma cells or cell pellets were frozen at -80 °C for RNA isolation.

3.10 Cells and cell culture

Cells were cultured in the incubator at 37 °C, 100% saturated humidity and 5% CO_2. The 2E10 NKT hybridoma cell line was generated and kindly provided by Dashtsoodol Nyambayar, M.D., Ph.D (Department of Hematology and Medical Oncology, Klinikum rechts der Isar and TranslaTUM Cancer Center, Technische Universität München, München, Germany) [151]. This cell line was cultured in RPMI 1640 medium supplemented with 10% FBS, 2 mM L-glutamine, 1 mM sodium pyruvate, 1% penicillin/streptomycin and 10 mM HEPES in 10 cm culture dishes.

3.11 Activation of 2E10 hybridoma cells

1.25 x 10^6 sorted DP T cells from pTa-$Cre^{wt/wt}$-*Lamtor2*$^{f/f}$, pTa-$Cre^{ki/wt}$-*Lamtor2*$^{wt/wt}$ or pTa-$Cre^{ki/wt}$-*Lamtor2*$^{f/f}$ mice we pre-incubated with 100 mM aGC for 1 h in a 96-well plate. Next, 2.5 x 10^5 2E10 NKT hybridoma cells were co-cultured with DP T cells to examine the ability of LAMTOR2-deficient DP thymocytes to stimulate IFN-γ release the 2E10 cells. DP T cells or 2E10 hybridoma cells served as controls. Supernatants were collected after 24 h of

incubation and production of IFN-γ was quantified by Enzyme-linked Immunosorbent Assay (ELISA).

3.12 Enzyme-linked Immunosorbent Assay

Levels of IFN-γ were determined by Enzyme-linked Immunosorbent Assay (Mouse IFN-gamma DouSet ELISA) and performed according to the manufacturer's instructions. Prior to detection 100 µl pre-warmed eBioscience™ TMB Solution (1X) were added per well. After ca. 20 min of incubation at RT in the dark, the reaction was stopped by adding 50 µl stop solution (1M H_3PO_4) to each well. Spectrometric analysis at 450 nm (Synergy H1 Hybrid Reader) was obtained and IFN-γ concentrations were calculated based on standard curves.

3.13 *In vivo* administration of aGC

In oder to analyze the ability of aGC presentation on DP T cells, 6-8 weeks old mice were injected intraperitoneally (i.p.) with 2 µg aGC in a final volume of 100 µl sterile PBS, supplemented with 0.5% Tween® 20 and 5.6% Sucrose, at day 0 and day 4. As controls, mice were injected with 100 µl diluent (sterile PBS + 0.5% Tween® 20 and 5.6% Sucrose). One hour after the second injection, mice were sacrificed and thymocytes, splenocytes and hepatocytes were isolated and washed with 10 ml 2% FBS in PBS. Red blood cells were lysed with 1 ml RBC Lysis Buffer at RT for 5 min. Cells were washed with 10 ml 2% FBS in PBS and resuspended in 1 ml 2% FBS in PBS. 1 x 10^7 cells/sample were stained with cell surface antibodies/tetramer (Table 17 and Table 5, respectively) for 30 min at 4 °C. NKT cell populations and aGC-loading onto CD1d was analyzed by flow cytometry.

3.14 *In vivo* bromodeoxyuridine incorporation

To analyze iNKT cell proliferation, 6-8 weeks old mice were injected i.p. with 1 mg/ml bromodeoxyuridine (BrdU), diluted 100 µl sterile PBS, followed by 2 days of supplying BrdU in drinking water (1 mg/ml BrdU, light protected, daily water change). Mice were sacrificed, thymocytes were isolated, washed with 10 ml 2% FBS in PBS and 1 x 10^7 cells/sample were stained with cell surface

antibodies/tetramer and Fixable Viability Stain (FVS) (Table 5 and 17) for 30 min at 4 °C. Next, cells were prepared for BrdU incorporation analysis using the BrdU Flow Kit according to the manucaturer's instructions (BD Pharmingen). Briefly, cells were fixed, permeabilized, treated with DNase, and stained with anti-BrdU-APC. The BrdU incorporation was measured by flow cytometry at a speed of 800 events/sec.

3.15 *In vivo* acute thymic involution (ATI) mouse model

To investigate, whether iNKT cells contribute to thymic inflammation, we applied a toxin-induced acute thymic involution (ATI) mouse model, using carbon tetrachloride (CCL_4), as previously described by Scholten et al. [152]. For the induction of an ATI, mice were injected once with 1 ml CCl_4/kg body weight i.p., diluted in a final volume of 100 µl sterile corn oil. 48 hours after the injection, mice were weighted and sacrificed. The thymus was isolated, weighted and processed to single cell suspensions. Cells were washed with 1 ml 2% FBS in PBS and up to 2 x 10^7 cells/sample were stained in 100 ul 2 % FBS in PBS for FACS analysis.

3.16 Statistical analysis

Statistical analysis was performed using Prism software (GraphPad Software Inc.). Differences between groups were analyzed by ANOVA or Student's *t*-test. Data are presented as mean ± standard deviation. Results showing a *p*-value <0.05 were considered statistically significant.

4. Results

4.1 Generation of pTα-Cre-*Lamtor2*$^{flox/flox}$ mice

To investigate the role of LAMTOR2 during early T cell development, we generated *pTα-Cre-Lamtor2*$^{flox/flox}$ mice by crossing *pTa-Cre*$^{ki/wt}$ mice (Ptcra$^{tm1(icre)Hjf}$; C57BL/6J background, generated by Prof. Dr. Hans Jörg Fehling, Ph. D., provided by EMMA Mouse Repository, Dr. Susan Marschall) and *Lamtor2*$^{flox/flox}$ mice ([13], C57BL/6J background, provided by Prof. Dr. Lukas Alfons Huber, M.D.). These conditional KO mice exhibit a T cell-specific deletion of *Lamtor2*, starting at T cell developmental stage DN2/DN3 (Fig. 9A). Efficient *Lamtor2* deletion of mRNA was confirmed in CD3$^+$B220$^-$ and CD3$^-$B220$^-$ T cells in the thymus as well as in CD3$^+$B220$^-$ T cells in the lymph nodes (LN) of pTα-Cre-*Lamtor2*$^{fl/fl}$ mice by qPCR (Fig. 9B). Furthermore, LAMTOR2 protein was neither detectable in CD3$^+$B220$^-$ and CD3$^-$B220$^-$ thymic T cells nor CD3$^+$B220$^-$ T cells from LN of pTα-Cre-*Lamtor2*$^{fl/fl}$ mice by Western Blot analysis (Fig. 9C).

As mice with expression of the *Cre* recombinase lack one allele of the pre-TCRα gene (*ptrca*), which might lead to toxicity, off-target effects or might have a direct effect on T cell development, we used both pTa-Cre$^{wt/wt}$-*Lamtor2*$^{f/f}$ and pTa-Cre$^{ki/wt}$-*Lamtor2*$^{wt/wt}$ mice as control mice in our studies. pTa-Cre$^{wt/wt}$-*Lamtor2*$^{f/f}$ control mice are referred to as WT mice, pTa-Cre$^{ki/wt}$-*Lamtor2*$^{wt/wt}$ control mice are referred to as Cre transgene control mice and pTa-Cre$^{ki/wt}$-*Lamtor2*$^{f/f}$ are referred to as KO mice in the further analyses.

Initial characterization of WT, Cre transgene control and KO mice revealed no significant differences of thymus weight and total thymocyte cell numbers in KO mice (2.60±0.87 g/10^3, 0.54±0.24 x10^7) compared to WT (3.51±1.31 g/10^3, 0.75±0.30 x10^7) and Cre transgene control (3.16±0.99 g/10^3, 0.63±0.22 x10^7) mice (Fig. 9D). Cre transgene control mice had only slightly but not significantly reduced thymus weight and total thymocyte cell numbers compared to WT mice.

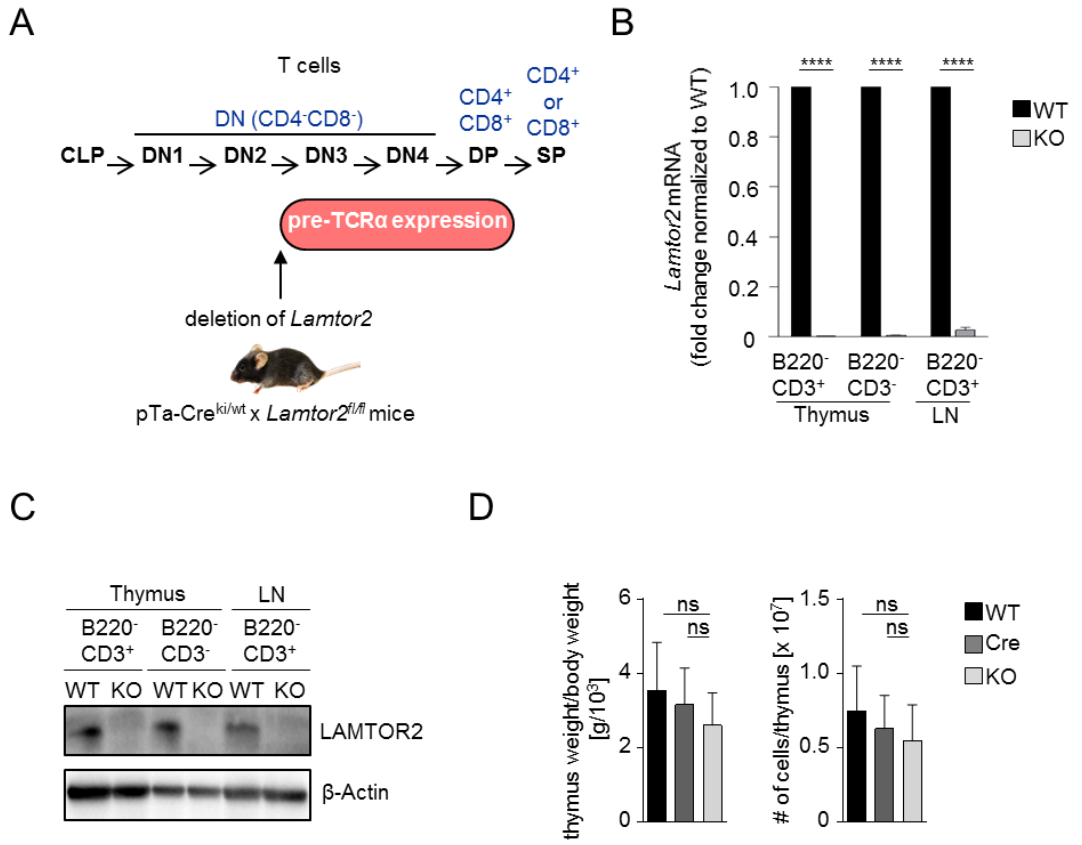

Figure 9: Generation of *pTaCre-Lamtor2*$^{fl/fl}$ mice. A) Schematic overview of the *pTaCre-Lamtor2*$^{fl/fl}$ mouse model. In this mouse model, deletion of *Lamtor2* is induced specifically in T cells upon expression of pre-TCRα at developmental stage DN2-DN3. B) qPCR for analysis of mRNA deletion efficiency of *Lamtor2* in T cells of thymus and lymph nodes (LN) of *pTaCre-Lamtor2*$^{fl/fl}$ mice. *Lamtor2* mRNA was efficiently deleted in B220^{-}CD3^{+} and B220^{-}CD3^{-} thymic T cells as well as in B220^{-}CD3^{+} T cells in the lymph nodes. Data (mean ± SD) shown are calculated from 3 independent experiments with 2-4 mice per genotype. C) Western Blot for analysis of protein deletion efficiency of LAMTOR2 in T cells of thymus and LN of *pTaCre-Lamtor2*$^{fl/fl}$ mice. LAMTOR2 protein was not detected in B220^{-}CD3^{+} and B220^{-}CD3^{-} thymic T cells and in B220^{-}CD3^{+} T cells from lymph nodes. Data are representative of 3 independent experiments with 2-4 mice per genotype. D) Analysis of the thymus weight and numbers of thymocytes/thymus in *pTaCre-Lamtor2*$^{fl/fl}$ mice. Thymus weight per body weight and the total number of cells per thymus did not differ significantly between WT (*pTaCre*$^{wt/wt}$*-Lamtor2*$^{fl/fl}$), Cre (*pTaCre*$^{ki/wt}$*-Lamtor2*$^{wt/wt}$) and KO (*pTaCre*$^{ki/wt}$*-Lamtor2*$^{fl/fl}$) mice. Data (mean ± SD) shown are calculated from 3-5 independent experiments with 2-4 mice per genotype.

4.2 LAMTOR2 is dispensable for conventional T cell development after stage DN2/3

Immunophenotypic analysis of conventional T cell progenitor subsets revealed normal proportions of double negative (DN) CD4^{-}CD8^{-} committed T-cell

precursor, double positive (DP) $CD4^+CD8^+$ T cells, $CD4^+$ single positive (CD4 SP) T cells, and $CD8^+$ single positive (CD8 SP) T cells of KO mice compared to WT and Cre transgene control mice (Fig. 10A and 10B). We also assessed the earliest developmental stages DN1-DN4 by analysis of the expression of CD25 and CD44 antigens on DN cells (DN1: $CD44^+CD25^-$, DN2: $CD44^+CD25^+$, DN3: $CD44^-CD25^+$, DN4: $CD44^-CD25^-$). DN1-DN3 early T cell developmental stages were similar in WT, Cre transgene control and KO mice. However, KO mice (1.60±0.66 $x10^6$) exhibited significantly more cells in stage DN4 compared to WT (0.67±0.35 $x10^6$) and Cre transgene control (0.76±0.43 $x10^6$) mice, but further conventional T cell development was not impaired, as shown in normal numbers of DP and SP cells (Fig. 10B). Therefore, we propose that LAMTOR2 is not required for conventional T cell development after early developmental stage DN2/DN3.

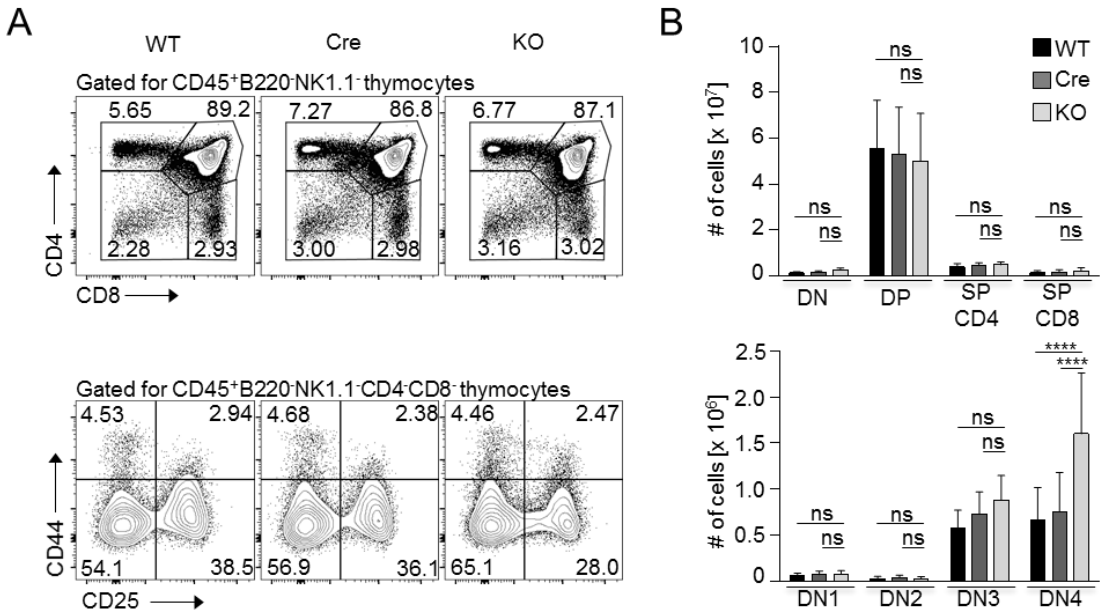

Figure 10: Normal conventional T cell development in *Lamtor2* KO mice. A) Representative flow cytometry based immunophenotyping of conventional T cell developmental stages in WT, Cre transgene control and *Lamtor2* KO mice. Data are representative of 3 independent experiments with 2-4 mice per genotype. B) Quantification of absolute numbers of conventional T cells in each developmental stage in WT, Cre transgene control and KO mice. *Lamtor2* KO mice exhibit a significantly increased total number of T cells in developmental stage DN4 as compared with WT and Cre transgene control mice, but no significant differences in DP, CD4 SP and CD8 SP were observed. Data (mean ± SD) shown are calculated from 3 independent experiments with 2-4 mice per genotype.

4.3 LAMTOR2 is required for thymic iNKT cell development

iNKT cells specifically bind to glycolipid-loaded CD1d tetramers (e.g., PBS57/CD1d tetramer, provided by the NIH tetramer core facility [50]), which can be used to uniquely identify them. Flow cytometry analysis showed a significant reduction of PBS57/CD1d tetramer$^+$TCRβ$^+$ iNKT cells in the thymus, spleen and liver of *Lamtor2* KO mice (0.01±0.01%, 0.01±0.01%, 0.17±0.20%) compared to WT (0.53±0.22%, 0.62±0.16%, 4.92±2.08%) and Cre transgene control (0.60±0.29%, 0.57±0.28%, 3.86±1.87%) mice (Fig. 11A and 11B), suggesting that LAMTOR2 is required for iNKT cell development.

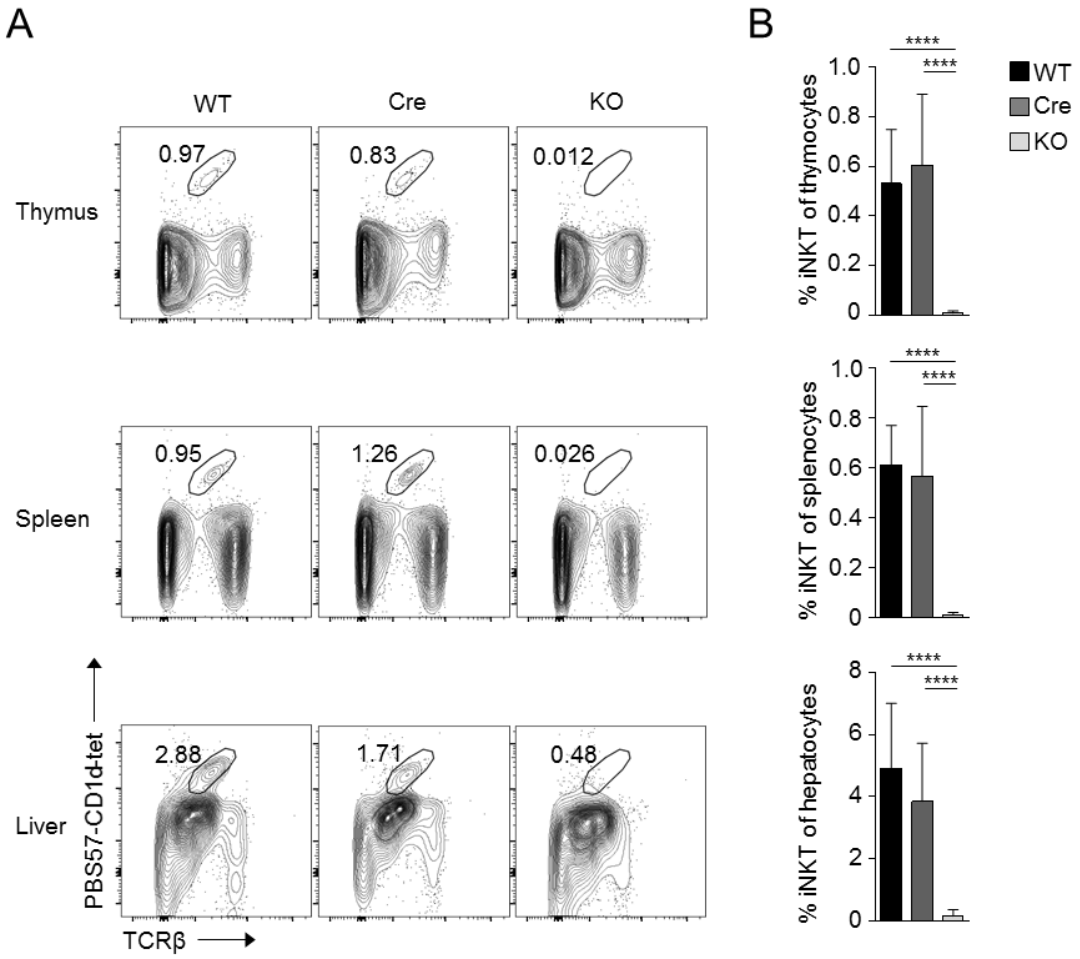

Figure 11: Impaired iNKT cell development in *Lamtor2* KO mice. A) Representative flow cytometry analysis of iNKT cell proportions in thymus, spleen and liver of WT, Cre transgene control and *Lamtor2* KO mice (n = 3 experiments, 2-4 mice per genotype). B) Quantification of iNKT cell proportions as percentage of whole thymocytes/splenocytes/hepatocytes in WT, Cre transgene control and *Lamtor2* KO mice. Proportions of iNKT cells are significantly reduced in thymus and peripheral organs in *Lamtor2* KO mice. Data (mean ± SD) shown are calculated from 3 independent experiments with 2-4 mice per genotype.

4.4 Rearrangement of invariant TCR is intact in LAMTOR2-deficient T cells

iNKT cells express a limited repertoire of invariant TCRs [48]. Each TCR contains a single Vα14 and Jα18 DNA segment combined with one of three Vβ segments (Vβ8, Vβ2, or Vβ7). To test whether LAMTOR2 is required for the rearrangement of the Vα14 to the Jα18 gene segment at the $CD4^+CD8^+$ DP developmental stage, we quantified the expression levels of *Vα14-Jα18* transcripts in sorted DP T cells, whole thymocytes and sorted splenic B cells by qPCR (Fig. 12). mRNA levels of *Vα14-Jα18* transcripts in DP T cells were normal in KO mice, suggesting that TCR rearrangement at the DP stage remains intact and iNKT lineage commitment has successfully occurred in the absence of LAMTOR2. However, *Vα14-Jα18* transcripts were significantly reduced in whole thymocytes of *Lamtor2* KO mice (fold change 0.38±0.16), compared to WT (fold change 6.48±3.60) and Cre transgene (fold change 8.35±4.03) controls, which reflects the strong overall reduction of thymic iNKT cell numbers in *Lamtor2* KO mice (positive control). *Vα14-Jα18* transcripts were undetectable in sorted splenic B cells in all samples, confirming qPCR primer specificity (negative control). In summary, our data suggests that LAMTOR2 is not required for TCR rearrangement in iNKT cells.

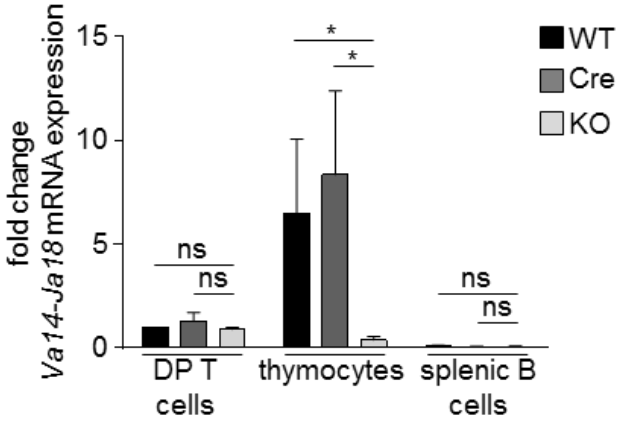

Figure 12: *Va14-Ja18* TCR rearrangement is normal in *Lamtor2* KO mice. qPCR analysis showed that *Va14-Ja18* mRNA expression in sorted DP T cells is not altered in *Lamtor2* KO mice, indicating functional *Va14-Ja18* TCR rearrangement. Reduced amounts of *Va14-Ja18* mRNA in whole thymocytes in *Lamtor2* KO mice reflect reduced overall numbers of thymic iNKT cells in *Lamtor2* KO mice. As a control,

sorted splenic B cells from WT, Cre transgene control and *Lamtor2* KO mice were tested negative for *Va14-Ja18* mRNA expression. Data (mean ± SD) shown are calculated from 3 independent experiments with 2-4 pooled mice per genotype.

4.5 iNKT cell development in LAMTOR2-deficient mice is blocked at early developmental stages

To investigate which step of iNKT cell development is affected by deletion *of Lamtor2*, we systematically analyzed the developmental stages during iNKT cell maturation. First, positively selected iNKT cells downregulate CD4 and CD8 and become DP^{dull} cells, before they move on to become $CD4^+$ or DN iNKT cells [150,153-155]. Flow cytometric analysis revealed reduced proportions of CD1d:PBS-57-tetramer$^+$TCRβ$^+$ iNKT cells in the DP^{dull} gate in *Lamtor2* KO mice (Fig. 13A and 13B), suggesting that positive selection of iNKT cells might be impaired. Next, we analyzed iNKT cell developmental stage 0 (ST0: CD1d:PBS-57-tetramer$^+$TCRβ$^+$CD24$^+$), stage 1 (ST1: CD1d:PBS-57-tetramer$^+$TCRβ$^+$CD24$^-$CD44^{lo}NK1.1$^-$), stage 2 (ST2: CD1d:PBS-57-tetramer$^+$TCRβ$^+$CD24$^-$CD44^{hi}NK1.1$^-$) and stage 3 (ST3: CD1d:PBS-57-tetramer$^+$TCRβ$^+$CD24$^-$ CD44^{hi}NK1.1$^+$). Whereas frequencies of iNKT cells in developmental stages ST0, ST1, and ST2 were increased in *Lamtor2* KO mice, proportions of iNKT cells in ST3 were significantly reduced (Fig. 13C and 13D). Quantification of absolute numbers of iNKT cells in the individual stages revealed strongly reduced numbers of ST2 (WT: 0.21±0.10 x10^5, Cre: 0.22±0.12 x10^5, KO: 0.0022±0.0010 x10^5) and ST3 (WT: 3.28±0.99 x10^5, Cre: 4.12±1.56 x10^5, KO: 0.0003±0.0008 x10^5) iNKT cells, indicating that cells do not develop beyond ST1 in *Lamtor2* KO mice (Fig. 13E). Therefore, we propose that LAMTOR2 plays an important role in positive selection and/or early iNKT cell development.

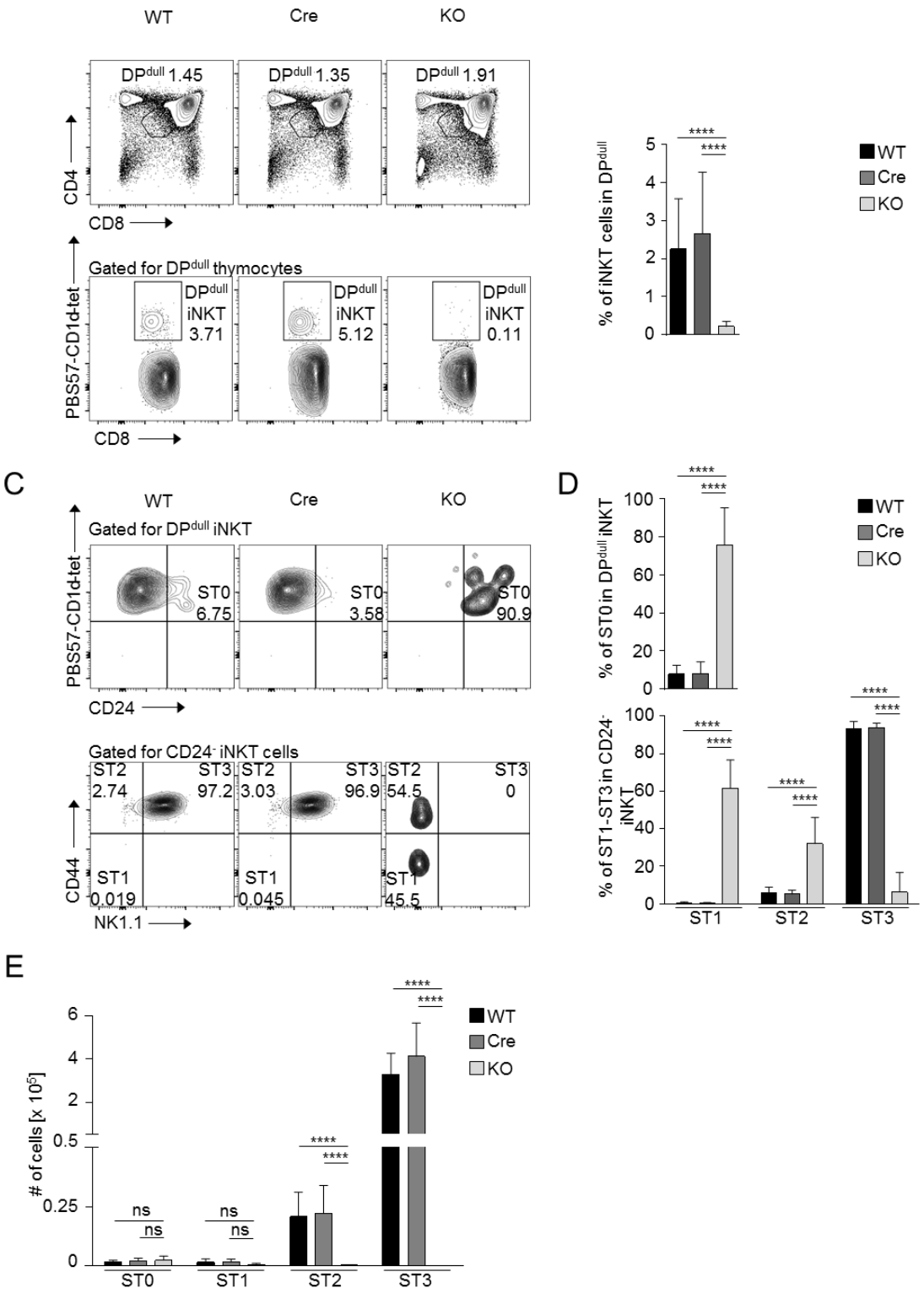

Figure 13: iNKT cells of *Lamtor2* KO mice do not develop beyond developmental stage ST1. A) Flow cytometry analysis of proportions of DP^{dull} iNKT cells in thymus of *Lamtor2* KO mice. Data are representative of 4 independent experiments with 2-4 mice per genotype. B) Quantification of proportions of thymic DP^{dull} iNKT cells in WT, Cre transgene control and *Lamtor2* KO mice. *Lamtor2* KO mice exhibit reduced proportions of DP^{dull} iNKT cells. Data (mean ± SD) shown are calculated from 4 independent experiments with 2-4 mice per genotype. C) Proportions of developmental stages ST0, ST1, ST2 and ST3 in WT, Cre transgene control and

Lamtor2 KO mice. Data are representative of 4 independent experiments with 2-4 mice per genotype. D) Quantification of proportions of thymic iNKT cells in ST0-ST3 in WT, Cre transgene control and *Lamtor2* KO mice. *Lamtor2* KO mice exhibit increased proportions of cells in developmental stages ST0, ST1 and ST2, but reduced proportions of ST3 iNKT cells. Data (mean ± SD) shown are calculated from 4 independent experiments with 2-4 mice per genotype. E) Absolute numbers of iNKT cells in each stage (ST0-ST3). *Lamtor2* KO mice lack iNKT cells in ST2 and ST3. Data (mean ± SD) shown are calculated from 3 independent experiments with 2-4 mice per genotype.

4.6 aGC presentation of DP T cells is reduced in LAMTOR2-deficient mice leading to impaired positive selection of iNKT cells

Once the *Vα14-Jα18* rearrangement has occurred in a DP T cell, the lineage specified Vα14-Jα18-Vβ8/2/7 TCR allows its positive selection mediated by CD1d-presented glycolipids expressed on another DP T cell [39]. aGC is a synthetic glycolipid antigen and it is commonly used as a potent agonist to selectively activate iNKT cells [95]. To assess the ability of DP thymocytes to present αGC onto CD1d, we treated sorted DP thymocytes from WT, Cre transgene control and *Lamtor2* KO mice with αGC for the indicated time points and analyzed the surface expression of αGC-loaded CD1d using an antibody specifically detecting the αGC-CD1d complex (clone L363) by flow cytometry. Upon aGC stimulation for 24 h, we detected an increased proportion of αGC-CD1d-complex$^+$ DP T cells from WT (5.33%) and Cre transgene control (4.61%) mice, while DP T cells from *Lamtor2* KO mice (0.33%) failed to load aGC onto CD1d (Fig. 14A and 14B).

As a second line of evidence, we examined the ability of LAMTOR2-deficient DP thymocytes to stimulate IFN-γ release of an iNKT cell hybridoma cell line (2E10) upon aGC treatment (Fig. 14C). Co-cultivation of NKT hybridoma with WT and Cre transgene control DP T cells in the presence of aGC significantly increased IFN-γ release, compared to NKT hybridoma cells alone. In contrast, *Lamtor2* KO DP T cells failed to present aGC efficiently towards NKT hybridoma cells, which is reflected in reduced IFN-γ release measured by ELISA (WT: 0.59±0.16, Cre: 0.70±0.32, KO: 0.28±0.35, above NKT background (in fold change)).

Lipid antigen (e.g. aGC) presentation on DP T cells is crucial for positive selection of iNKT cells *in vivo* [49,156]. To assess the ability of DP thymocytes to present αGC onto CD1d *in vivo*, mice were injected with 2 µg aGC per mouse on day 0 and day 4 and sacrificed 1 hour after the second injection. We detected significantly increased proportions of αGC-CD1d-complex^{+} DP T cells in aGC-injected WT (fold change 2.05±0.77) and Cre transgene control (fold change 2.95±0.94) mice, compared to *Lamtor2* KO (fold change 0.69±0.20) mice (Fig. 14D and 14E).

Next, we determined the surface expression of overall CD1d on DP T cells *in vivo* upon i.p. injection of aGC by flow cytometry (Fig. 14F and 14G). CD1d mean fluorescence intensity (MFI) was slightly reduced in *Lamtor2* KO mice, compared to WT and Cre transgene control mice, but this effect was independent of aGC injection in all samples.

In summary, our *ex vivo* and *in vivo* studies show that aGC-loading onto CD1d is defective in DP T cells of LAMTOR2-deficient mice, suggesting that LAMTOR2 is critical for positive selection of iNKT cells.

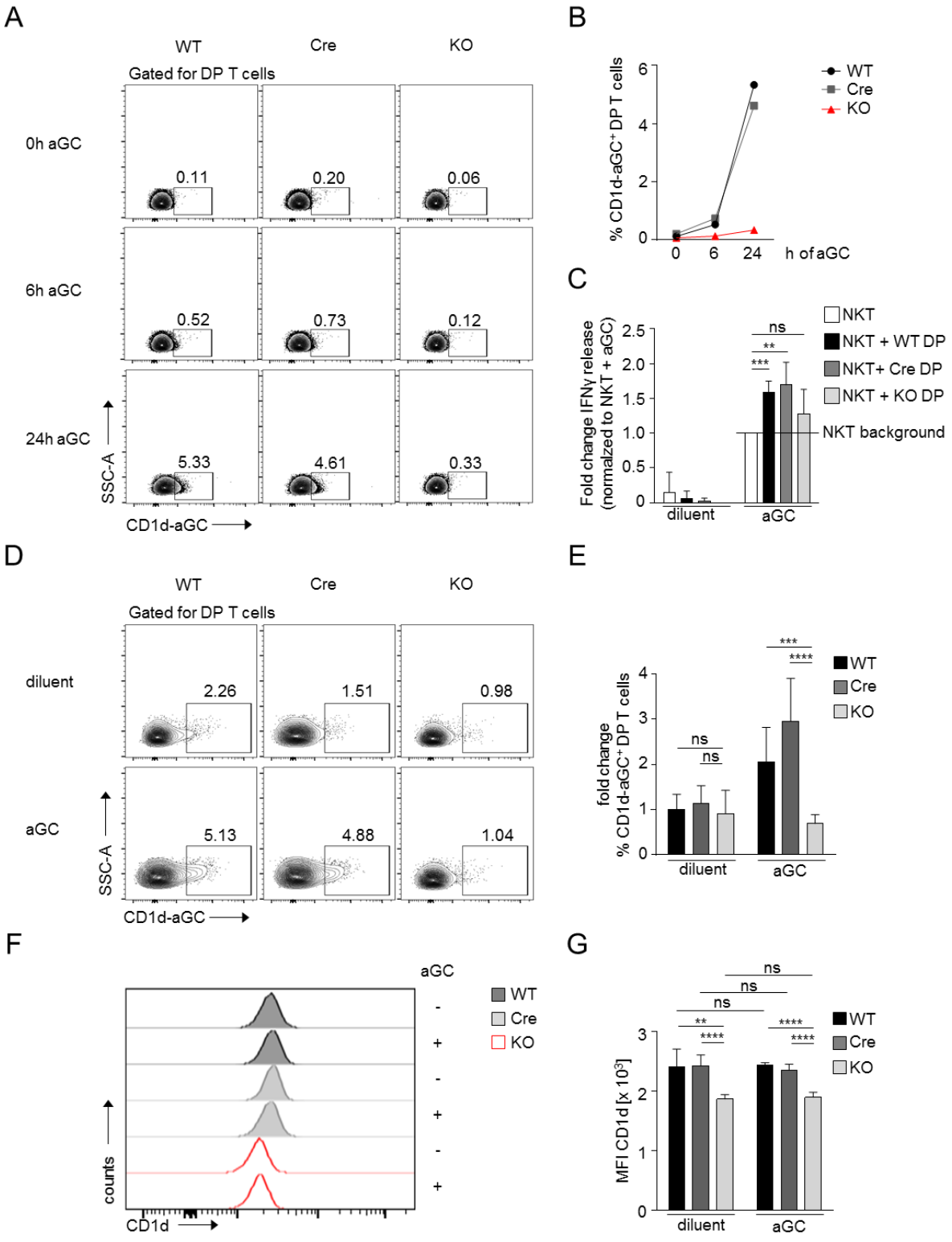

Figure 14: Impaired aGC presentation by LAMTOR2-deficient DP T cells. A) Representative flow cytometry analysis of *ex vivo* aGC-loading of DP T cells from WT, Cre transgene control and *Lamtor2* KO mice after aGC stimulation for indicated timepoints. aGC-loading onto CD1d was detected using a CD1d-aGC complex-specific antibody. Data are representative of 3 independent experiments with 2-4 pooled mice per genotype. B) Quantification of CD1d-aGC$^+$ DP T cells from WT, Cre transgene control and *Lamtor2* KO mice 0, 6 and 24 hours after stimulation with aGC

ex vivo. CD1d-aGC presentation on LAMTOR2-deficient DP T cells is reduced compared to WT and Cre transgene control DP T cells. Data are representative of 3 independent experiments with 2-4 pooled mice per genotype. C) IFN-γ release from 2E10 NKT hybridoma cell line upon co-cultivation with DP T cells (+/- aGC). Co-cultivation of NKT hybridoma with WT and Cre transgene control DP T cells in the presence of aGC led to significant increase in IFN-γ release. Co-cultivation of NKT hybridoma with KO cells only slightly increased IFN-γ release, compared with NKT hybridoma alone. Data (mean ± SD) shown are calculated from 4 independent experiments with 2-4 pooled mice per genotype. D) Representative flow cytometry analysis of *in vivo* aGC-loading of DP T cells in WT, Cre transgene control and *Lamtor2* KO mice two days after i.p. injection of 2 µg aGC. The CD1d-aGC complex was detected using a CD1d-aGC complex-specific antibody. Data are representative of 3 independent experiments with 2 mice per group. E) Quantification of CD1d-aGC$^+$ DP T cells from WT, Cre transgene control and *Lamtor2* KO mice injected with. 2 µg aGC (i.p.). *In vivo* CD1d-aGC presentation on LAMTOR2-deficient DP T cells is reduced compared to WT and Cre transgene control DP T cells. Data (mean ± SD) shown are calculated from 3 independent experiments with 2 mice per group. F) Representative flow cytometry analysis of CD1d overall surface expression on DP T cells in WT, Cre transgene control and KO mice +/-2 µg aGC injection. Data are representative of 3 independent experiments with 2 mice per group. G) Quantification of CD1d MFI in DP T cells in WT, Cre transgene control and KO mice +/-2 µg aGC injection. CD1d MFI in LAMTOR2-deficient DP T cells is reduced compared to WT and Cre transgene control cells. However, CD1d surface expression is not influenced by aGC injection in WT, Cre transgene control and KO mice. Data (mean ± SD) shown are calculated from 3 independent experiments with 2 mice per group.

4.7 LAMTOR2-deficient mice exhibit increased cell death at iNKT cell developmental stage ST1

In 4.6, we have shown that LAMTOR2 plays an important role in positive selection of iNKT cells. However, *Lamtor2* KO mice exhibit a few residual cells at ST0 and ST1 (Fig. 13E), which are developmental stages following positive selection. Therefore, we propose that LAMTOR2 plays another important role in iNKT cell development after positive selection. Potential causes for a reduction of iNKT cells at ST1 in KO mice could be reduced proliferation or increased cell death of developing iNKT cells. To investigate proliferation during early iNKT cell development, we performed *in vivo* BrdU incorporation assays. In parallel, we assessed cell death by using a fixable viability stain (FVS) before fixation of the harvested cells. Surprisingly, LAMTOR2-deficient mice incorporated more BrdU (35.31±6.45% BrdU$^+$) as compared to WT (6.62±1.73% BrdU$^+$) and Cre transgene control (5.89±1.20% BrdU$^+$) mice, when gating for all iNKT cells (Fig. 15A and 15B).

However, individual iNKT cell developmental stages are known to have different capacities of proliferation and cell death, e.g., iNKT cells at ST3 are non-cycling cells and show only very low frequencies of cell death compared to ST0, ST1 and ST2 [62]. To determine whether the observed differences were due to a different composition of cells in the individual developmental stages or due to increased proliferation and cell death in the individual stages, we gated on the specific ST0, ST1, ST2 and ST3 developmental stages. Interestingly, we observed similar proportions of $BrdU^+$ cells in the developmental stages ST0, ST1, ST2 and ST3 in WT, Cre transgene control and KO mice, indicating that thymic iNKT cell proliferation is normal in *Lamtor2* KO mice and increased overall proliferation of iNKT cells results from reduced proportions of non-cycling ST3 cells in KO mice.

Cell death analysis showed more cell death (FVS^+ cells) in the whole iNKT cell population in KO mice (FVS^+ cells: WT 4.74±2.07%, Cre 3.73±1.38%, KO 28.11±6.80%). Interestingly, analysis of the individual stages revealed significantly increased cell death at developmental stage ST1 in LAMTOR2-deficient mice (FVS^+ cells: WT 28.59±9.86%, Cre 20.69±9.25%, KO 53.47±18.35%). Therefore, we propose that increased cell death of iNKT cells in developmental stage ST1 impairs iNKT cell development beyond ST1 in the absence of LAMTOR2.

4.8 mTORC signaling in iNKT cell developmental stage ST1 is reduced in LAMTOR2-deficient mice

The transition from developmental stage ST1 to ST2 is critically regulated by mTORC1 signaling [157]. As LAMTOR2 has been shown to regulate mTORC signaling in a spatiotemporal fashion [11,12], we investigated mTORC1 signaling at ST0 and ST1 by Phosflow analysis of ribosomal protein S6 kinase beta-1 (p70S6K), a component of the mTORC1 pathway (Fig. 15C and 15D). Whereas the frequency of phospho-p70S6K(p-p70S6K)$^+$ cells in ST0 was low and comparable between WT, Cre transgene control and KO mice, the proportion of p-$p70S6K^+$ cells was reduced in LAMTOR2-deficient mice at ST1, compared to WT and Cre transgene control mice (WT: 72.57±15.08%,

Cre: 76.80±10.61%, KO: 52.40±14.81%. Based on these findings, we propose that LAMTOR2 may be critical for effective mTORC1 signaling at ST1.

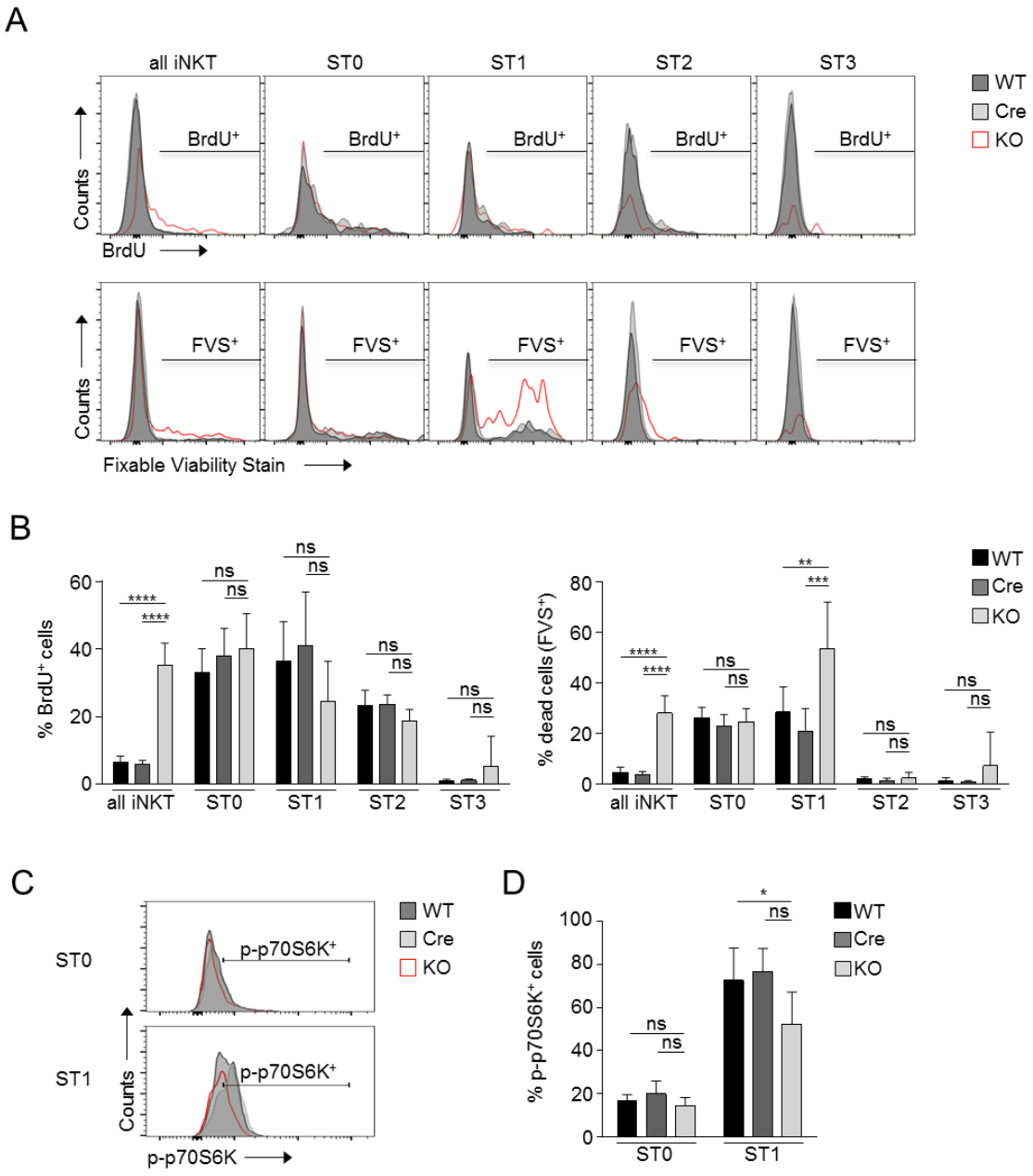

Figure 15: iNKT cells of LAMTOR2-deficient mice undergo more cell death and show reduced mTORC1 signaling at developmental stage ST1. A) Representative flow cytometry analysis of BrdU$^+$ and FVS$^+$ cells in all iNKT cells and the individual developmental stages in WT, Cre transgene control and Lamtor2 KO mice. Data are representative of 2 independent experiments with 3 mice per genotype. B) Quantification of BrdU+ and FVS+ cells in all iNKT cells and ST0-ST3. KO mice exhibit a significantly higher proportion of overall proliferating iNKT cells. However, no significant differences in proliferation were observed in the individual stages ST0-ST3. KO mice exhibit more cell death in the whole iNKT cell population, in particular reflected by increased cell death in developmental stage ST1. Data (mean ± SD) shown are calculated from 2 independent experiments with 3 mice per genotype. C) Representative Phosflow analysis of p-p70S6K in ST0 and ST1 iNKT cells from WT,

Cre transgene control and Lamtor2 KO mice. Data are representative of 3 independent experiments with 1-3 mice per genotype. D) Quantification of p-p70S6K$^+$ iNKT cells in developmental stage ST0 and ST1. The percentage of p-p70S6K$^+$ cells in ST0 is low in WT, Cre transgene control and KO mice. In ST1, more p-p70S6K$^+$ cells were detected in WT and Cre transgene control mice, compared to Lamtor2 KO mice. Data (mean ± SD) shown are calculated from 3 independent experiments with 1-3 mice per genotype.

4.9 *Lamtor2* KO mice are protected from CCL_4-induced acute thymic involution

Acute thymic involution (ATI) can be caused by infections, stress, pregnancy, malnutrition, chemotherapy and other toxins [158]. Glucocorticoids and pro-inflammatory cytokines have been shown to drive ATI, however, it is not known whether thymic iNKT cells contribute to it. To investigate if the lack of thymic iNKT cells protects *Lamtor2* KO mice from toxin-induced ATI, we administered CCl_4 (1 ml /kg body weight) i.p. and sacrificed the mice 48 hours later, as previously described [159]. Interestingly, thymus weight per body weight decreased significantly upon injection of CCl_4 in WT (-0.94±0.52 x10^3) and Cre transgene control (-1.76±0.46 x10^3) mice but not in *Lamtor2* KO (-0.39±0.44 x10^3) mice, indicating that loss of LAMTOR2 protects from developing ATI (Fig. 16A).

ATI is often characterized by remodeling the thymic T cell compartment associated with a loss of DP T cells [160,161]. Flow cytometric analysis of T cell progenitor stages revealed no difference in DP T cell proportions in WT KO mice, suggesting that conventional T cells do likely not play a role in driving ATI development (Fig. 16B and 16C). However, we observed a significant reduction of DP T cells in Cre transgene control mice, which might originate by chance from a low number of mice (2 mice per group in 2 independent experiments). Further studies are required to confirm this effect.

Interestingly, we found a significant increase in iNKT cell proportions after CCl_4 administration in WT (0.88±0.18% (+94% increase)), Cre transgene control (1.82±0.64% (+381% increase)) and KO (0.015±0.006% (+13878% increase)) mice (Fig. 16B and 16C), which indicates that iNKT cells play a role in inflammatory processes during development of ATI.

In summary, our studies suggest that lack of iNKT cells protects from ATI development in *Lamtor2* KO mice.

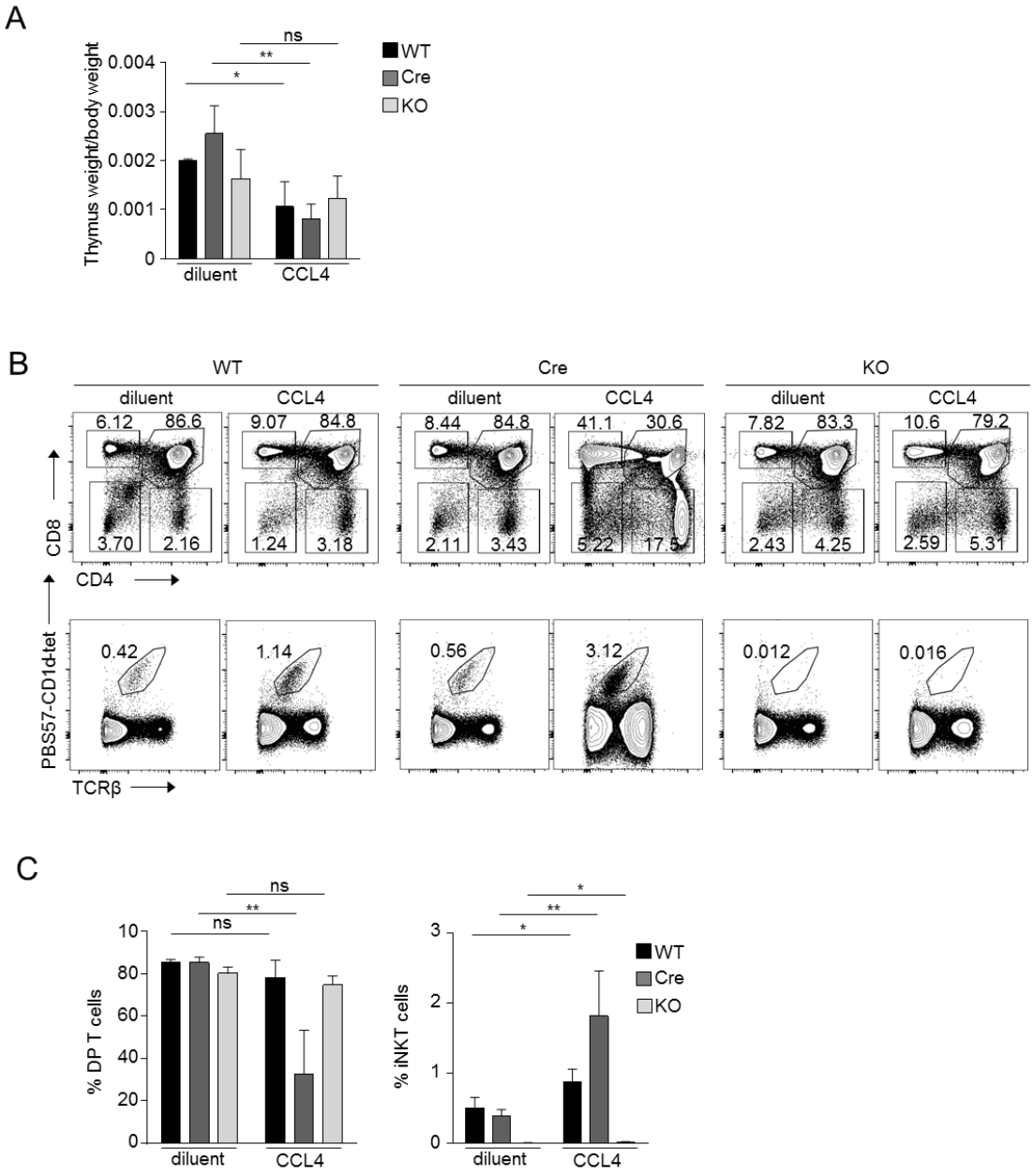

Figure 16: *Lamtor2* KO mice are protected from CCL_4-induced acute thymic involution (ATI). A) Thymus weight per body weight in WT, Cre transgene control and KO mice after i.p. administration of diluent control or 1 ml CCl_4/kg CCL4 for 2 days. WT and Cre transgene control mice but not KO mice lose thymus weight in response to CCl_4. Data (mean ± SD) shown are calculated from 2 independent experiments with 2 mice per group. B) Flow cytrometry analysis of conventional T cell Progenitor stages and thymic iNKT cell proportions upon CCl_4 injection in WT, Cre transgene control and KO mice. Data are representative of 2 independent experiments with 2 mice per group. C) Quantification of proportions of thymic DP T and iNKT cells from mice injected with diluent or CCl_4. DP T cells are significantly reduced in Cre transgene control mice in response to CCl_4, but not in WT and KO mice iNKT cells significantly increase in WT, Cre transgene control and KO mice after

CCl_4 injection. Data (mean ± SD) shown are calculated from 2 independent experiments with 2 mice per group.

4.10 Peripheral iNKT cells of *Lamtor2* KO mice do not respond to aGC-mediated activation

In previous reports, proportions of peripheral $CD44^+NK1.1^-$ iNKT cells increased in response to aGC injection [162,163]. The authors suggested an activation-induced downmodulation of NK1.1 surface receptors as a possible explanation. To investigate the function of LAMTOR2 in iNKT cells in peripheral aGC-mediated activation, mice were injected with 2 x 2 µg aGC/mouse (day 0 and day 4) and sacrificed 1 hour later for flow cytometry analysis.

Overall iNKT cell proportions in the thymus, spleen and liver did not increase in WT, Cre transgene control and KO mice upon aGC treatment (Figure 17A and 17B). However, WT and Cre transgene control mice, but not KO mice, exhibited an altered iNKT cell compartment, as detected by an increased proportion of $CD44^+NK1.1^-$ iNKT cells in spleen (WT: 59.88±4.88%, Cre: 69.28±5.57% KO: 35.35±7.74%) and liver (WT: 58.52±17.92%, Cre: 61.77±10.85% KO: 6.80±6.62%) in response to aGC (Fig. 18A and 18B). Thus, we conclude that LAMTOR2 might play an important role aGC-induced activation and effector function of iNKT cells in peripheral organs.

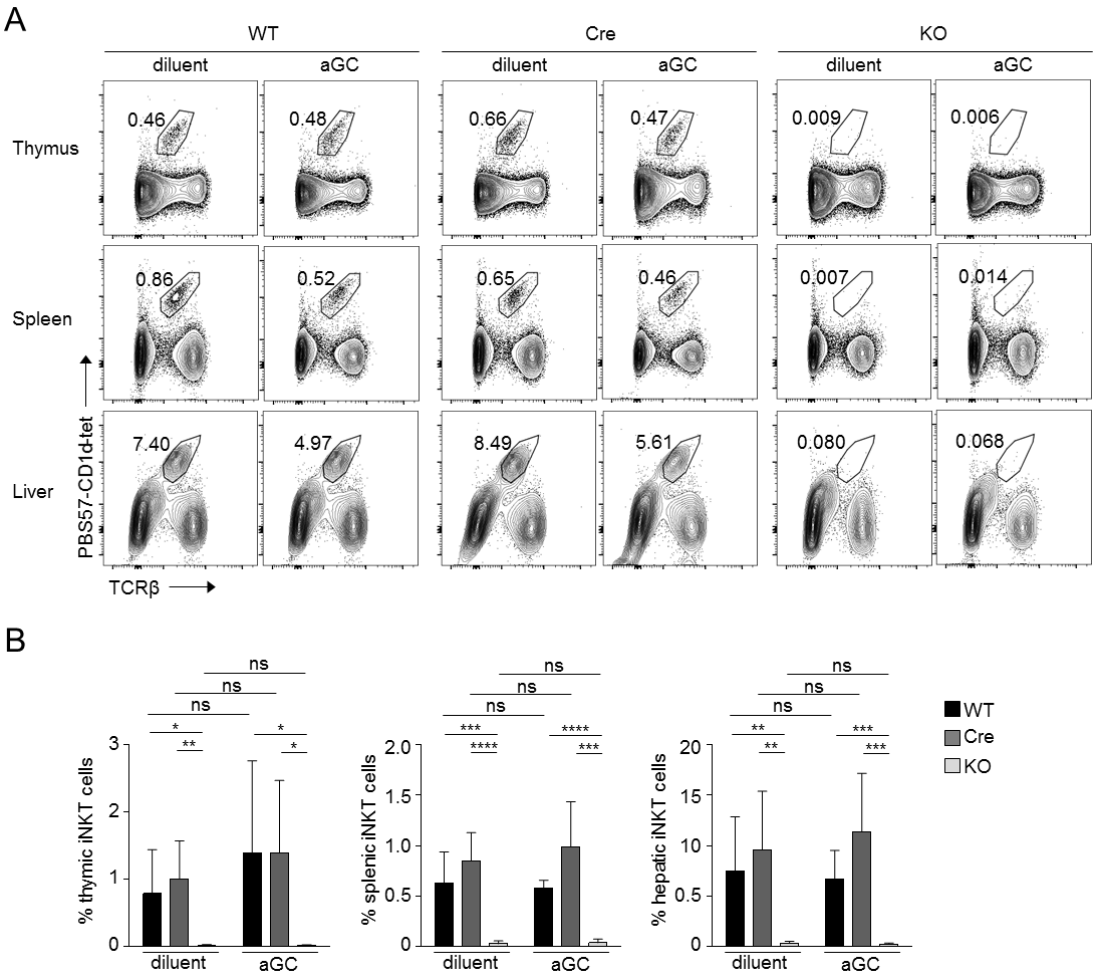

Figure 17: Proportions of iNKT cells in WT, Cre transgene control and *Lamtor2* KO mice do not change upon aGC injection. A) Representative flow cytometry analysis of iNKT cell proportions in thymus, spleen and liver of WT, Cre transgene control and *Lamtor2* KO mice after i.p. injection of diluent or aGC. Data are representative of 3 independent experiments with 2 mice per group. B) Quantification of iNKT cell proportions as percentage of whole thymocytes/splenocytes/hepatocytes in WT, Cre transgene control and *Lamtor2* KO mice. Proportions of iNKT cells are significantly reduced in thymus and peripheral organs in *Lamtor2* KO mice, but aGC injection does not affect iNKT cell proportions in all genotypes. Data (mean ± SD) shown are calculated from 3 independent experiments with 2 mice per genotype.

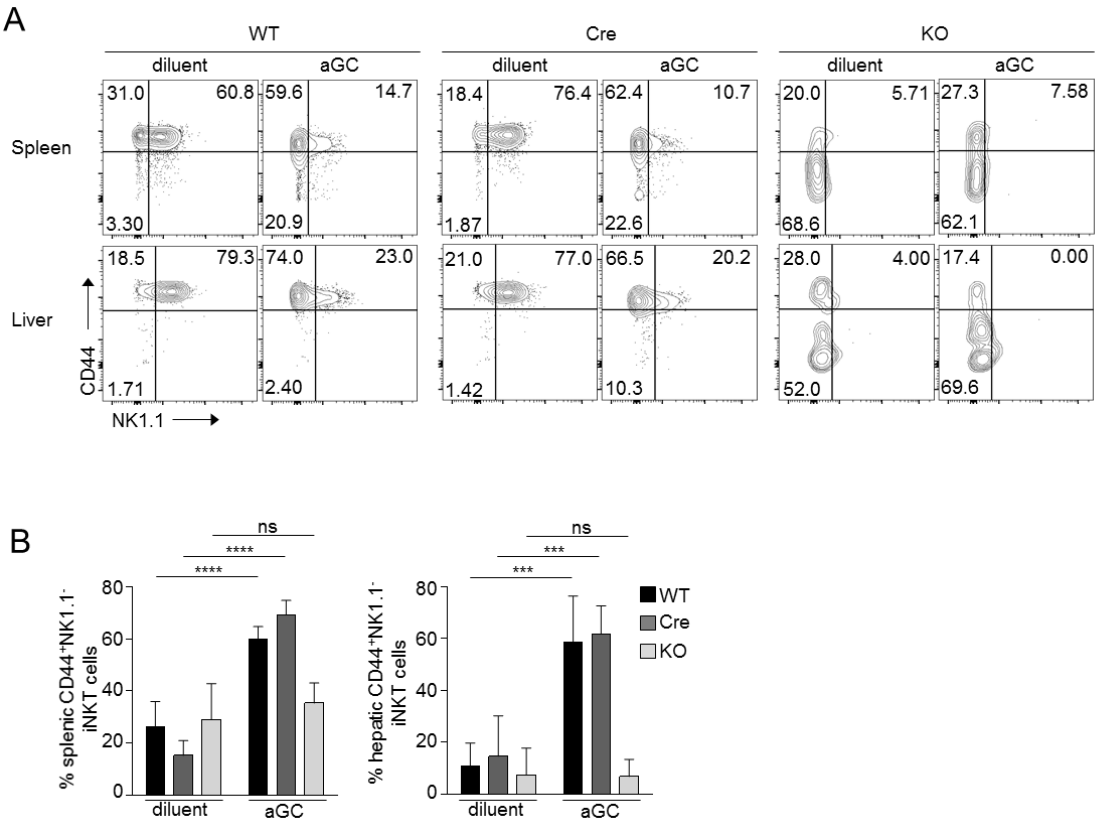

Figure 18: *Lamtor2* KO mice do not modulate their peripheral iNKT cell compartment upon aGC injection. A) Representative flow cytometry analysis of splenic and hepatic $CD44^{-}NK1.1^{-}$, $CD44^{+}NK1.1^{-}$ and $CD44^{+}NK1.1^{+}$ iNKT cells after i.p. injection of diluent or aGC. Data are representative of 3 independent experiments with 2 mice per group. B) Quantification of $CD44^{+}NK1.1^{-}$ iNKT cells in spleen and liver upon diluent/aGC injection. Consistently with previous reports, the peripheral iNKT compartment was modulated towards $CD44^{+}NK1.1^{-}$ iNKT in WT and Cre transgene control mice after treatment with aGC. In contrast, *Lamtor2* KO mice did not respond to aGC. Data (mean ± SD) shown are calculated from 3 independent experiments with 2 mice per group.

5. Discussion

5.1 LAMTOR2 regulates iNKT cell development in mice

Previous studies showed that LAMTOR2 is a crucial regulator of mTORC1 and ERK signaling on late endosomes in various cells of the immune system [9-12,127]. It is involved in many fundamental cellular processes including motility, lipid biosynthesis, cell growth, apoptosis, proliferation, protein synthesis, differentiation, and autophagy [15-19].

To the best of our knowledge, the presented PhD thesis provides the first evidence that LAMTOR2 plays a fundamental role in regulating iNKT cell development in mice. Using conditional KO mice that exhibit a T cell-specific deletion of *Lamtor2*, starting at T cell developmental stage DN2/DN3, we observed a significant reduction of iNKT cells in the thymus, spleen and liver, while conventional T cell development remained intact (Fig. 10, 11). Therefore, LAMTOR2 seems to have a critical function in iNKT cells, while it is not essential for conventional T cell development. To investigate the role for LAMTOR2 in iNKT cells, we systematically analyzed the three major steps during iNKT cell development: (i) iTCR rearrangement for lineage commitment, (ii) positive selection, and (iii) the expansion and differentiation of positively selected iNKT cells [44,154].

5.2 LAMTOR2 mediates glycolipid presentation for positive selection of iNKT cells

Our data demonstrated that LAMTOR2 plays an important role in the presentation of glycolipids onto CD1d molecules on DP thymocytes to mediate positive selection of iNKT cells. Using an aGC-CD1d complex-specific antibody, we found reduced aGC-loading on DP T cells of *Lamtor2* KO mice *in vivo* and *ex vivo* (Fig. 13 A, B, D, E). Furthermore, sorted LAMTOR2-deficient DP T cells failed to induce efficient aGC-mediated IFN-γ release in NKT hybridoma cells (Fig. 13 C). These results are consistent with reduced proportions of DP^{dull} iNKT cells, which are the first upcoming iNKT cells after positive selection, in *Lamtor2* KO mice (Fig. 12 A, B). Our results support the

paradigm that CD1d-mediated glycolipid antigen presentation on DP T cells is crucial for iNKT cell positive selection [36,56,57,59]. Glycolipid antigens are processed in the endo-lysosomal system prior to the presentation towards iNKT cells. Endosomal adaptor proteins (AP1, AP3) support endo-lysosomal trafficking of glycolipid antigens [33,36,61,156], however, this process seems to involve more adaptor proteins. Previously, our laboratory and others described that LAMTOR2 regulates endosomal trafficking of lysosomal-related organelles (e.g., azurophilic and lytic granules, and melanosomes) in neutrophils, CTLs and melanocytes [22,30,164-166]. These findings are in line with our results and point towards a putative role of LAMTOR2 during endo-lysosomal trafficking of glycolipid antigens in DP T cells. Furthermore, our findings provide insights why the development of conventional T cells is not affected in *Lamtor2* KO mice, because processing of protein antigens and presentation on MHC complexes towards precursor conventional T cells for positive selection does not involve the endo-lysosomal system (MHCI) or a different endo-lysosomal trafficking pathway (MHCII) [36,49,167]. Although our results demonstrate that LAMTOR2 is involved in the presentation of glycolipid antigens by DP T cells towards iNKT cell precursors, further work is needed to determine the detailed mechanisms of LAMTOR2-mediated intracellular trafficking and loading of glycolipid antigens onto CD1d of DP T cells.

5.3 LAMTOR2 is crucial for iNKT cell differentiation from ST1 to ST2 cells

Our data showed that LAMTOR2 plays a fundamental role in the transition from iNKT developmental stage ST1 to ST2 after positive selection. Using flow cytometry, we found significantly reduced numbers of absolute ST2 and ST3 iNKT cells in thymi of *Lamtor2* KO mice (Fig. 12 E). Although analysis of proliferation did not reveal any differences, cell death was increased in ST1 iNKT cells of LAMTOR2-deficient mice (Fig. 14 B), providing an explanation for reduced absolute numbers in subsequent developmental stages. Furthermore, our results showed reduced phosphorylation of p70S6K, a component of the mTORC1 signaling pathway, in ST1 iNKT of *Lamtor2* KO mice (Fig. 14 C, D). This finding raises the question whether LAMTOR2

regulates mTORC1 signaling during early iNKT cell development. mTORC1 signaling has been shown to be crucial for the transition of developmental stage ST1 to ST2 [81,157]. Moreover, previous mouse studies have demonstrated that LAMTOR2 regulates mTORC1 signaling in various cell types, e.g. LCs, DCs and podocytes [14,20,22]. Based on these data, it is suggestive that LAMTOR2 plays an important role in mTORC signaling and survival during early iNKT cell development. Potentially, LAMTOR2 regulates mTORC signaling in a spatiotemporal fashion, as spatiotemporal regulation of signaling pathways by LAMTOR2 has been described previously [11,12]. Therefore, timing and localization of signaling molecules in the mTORC1 pathway should be studied in more detail in ST0 and ST1 iNKT cells. However, at this point, we cannot exclude the confounding influence of other signaling pathways, which might also be affected by *Lamtor2* deletion. For example, in epidermal cells and myeloid cells LAMTOR2 plays important roles in ERK and/or signal transducer and activator of transcription 3 (STAT3) signaling ([13], unpublished data).

It would be interesting to investigate whether loss of LAMTOR2 results in reduced iTCR signaling as well, because it has been previously shown that iTCRs on iNKT precursor cells send stronger signals subsequently to positive selection for their survival and proliferation compared to signals from the TCR on conventional T cells [168-170]. This could be another explanation why LAMTOR2-deficient mice exhibit a defective iNKT cell development, but normal conventional T cell development. Future work on testing the impact of *Lamtor2* deletion on different signaling pathways mediating survival of precursor iNKT cells is needed.

5.4 The contributions of both LAMTOR2-regulated processes (positive selection and ST1-ST2 transition) to the observed phenotype need to be determined

Our results point towards a putative role of LAMTOR2 in both the glycolipid presentation for positive selection and the transition from ST1 to ST2 precursor iNKT cells. It is tempting to speculate that the addition of both defective mechanisms leads to the loss of mature iNKT cells in the thymus and

peripheral organs upon deletion of LAMTOR2. However, our current data does not provide exact information on the contributions of each of the processes to this phenotype. For example, analysis of mixed bone marrow chimera would provide crucial insights into these LAMTOR2-regulated processes for iNKT cell development in mice.

5.5 iNKT cells exhibit a relevant function in a toxin-induced ATI mouse model

We observed that *Lamtor2* KO mice with lack of iNKT cells in the thymus are protected from CCL_4-induced ATI (Fig. 15 A), whereas increased ATI in WT and Cre transgene control mice correlated with increased iNKT cell numbers (Fig. 15 B, C). These findings support previous reports, that ATI is driven by inflammatory processes in the thymus [161,171], but the mechanisms of ATI development are poorly understood. Our work offers new insights into the type of immune cells driving inflammation during ATI. However, further confirmatory and mechanistic studies on the contribution of iNKT cells to ATI development are needed. It would be interesting to investigate whether iNKT cells are involved in ATI development irrespectively of the trigger for ATI or if this mechanism is specific for CCL_4-induced ATI. Gaining a better understanding on the development of ATI might have therapeutic implications for humans suffering from ATI in response to toxins, viral infections, malnutrition or chemotherapy.

5.6 The peripheral iNKT cell response is defective in LAMTOR2-deficient mice

Finally, we analyzed the activation-induced downregulation of NK1.1 upon aGC injection in peripheral iNKT cells. Our studies showed that the few residual splenic and hepatic *Lamtor2* KO iNKT cells did not respond towards aGC (Fig. 16 A, B). However, we cannot exclude that the few remaining detected iNKT cells in spleen and liver are not actually iNKT cells, but a few unspecifically stained cells detected by flow cytometry, which is a limitation of our used method. Another explanation could be that the few remaining iNKT cells are WT cells, due to an incomplete conditional KO of *Lamtor2*.

State-of-the-art single RNA-sequencing approaches might shed light on whether these residual cells are true/can be categorized as iNKT cells. It is tempting to speculate that the strong reduction of absolute numbers of iNKT cells and unresponsiveness of the few remaining iNKT cells in the spleen and liver are relevant for various iNKT cell-mediated immune conditions in mice and humans. iNKT cells bridge the innate and adaptive immune system and have been implicated in various immunological processes against microorganisms [96]. They can promote anti-tumor immunity and autoimmune conditions, however immune-modulating functions of iNKT cells have been reported as well [38,108]. For example, during development of liver disease, iNKT cells can play protective or pathogenic roles in mouse models of CCl4-induced liver fibrosis [144,145]. To determine the impact of the lack of iNKT cells in the periphery of LAMTOR2-deficient mice, modeling human diseases in mice, for example applying a CCl_4-induced liver fibrosis mouse model, would shed light on these questions.

5.7 Conclusions and outlook

In summary, we have uncovered a fundamental role for LAMTOR2 in thymic iNKT cell development and function. However, additional work has to be done to clearly define the mechanistic role of LAMTOR2 during iNKT cell development and peripheral effector function. Furthermore, studies with human material are needed to confirm that our findings translate to humans. Our observations in mice indicate LAMTOR2 as a potential therapeutic target for humans suffering from ATI or other iNKT cell-driven pathological conditions, e.g., liver fibrosis and auto-inflammatory diseases.

6. References

1. Sehnal D Bittrich S (2021) Mol* Viewer: modern web app for 3D visualization and analysis of large biomolecular structures. 49: W431-w437.

2. Berman HM, Westbrook J, Feng Z, Gilliland G, Bhat TN, Weissig H *et al.* (2000) The Protein Data Bank. Nucleic Acids Res 28: 235-42.

3. Araujo MEGd, Naschberger A, Fürnrohr BG, Stasyk T, Dunzendorfer-Matt T, Lechner S *et al.* (2017) Crystal structure of the human lysosomal mTORC1 scaffold complex and its impact on signaling. Science 358: 377-381.

4. Wunderlich W, Fialka I, Teis D, Alpi A, Pfeifer A, Parton RG *et al.* (2001) A novel 14-kilodalton protein interacts with the mitogen-activated protein kinase scaffold mp1 on a late endosomal/lysosomal compartment. J Cell Biol 152: 765-76.

5. Schaab C, Geiger T, Stoehr G, Cox J Mann M (2012) Analysis of high accuracy, quantitative proteomics data in the MaxQB database. Mol Cell Proteomics 11: M111.014068.

6. Kolker E, Higdon R, Haynes W, Welch D, Broomall W, Lancet D *et al.* (2012) MOPED: Model Organism Protein Expression Database. Nucleic acids research 40: D1093-D1099.

7. Schmidt T, Samaras P, Frejno M, Gessulat S, Barnert M, Kienegger H *et al.* (2017) ProteomicsDB. Nucleic Acids Research 46: D1271-D1281.

8. Basha O, Barshir R, Sharon M, Lerman E, Kirson BF, Hekselman I *et al.* (2017) The TissueNet v.2 database: A quantitative view of protein-protein interactions across human tissues. Nucleic Acids Res 45: D427-d431.

9. Teis D, Wunderlich W Huber LA (2002) Localization of the MP1-MAPK scaffold complex to endosomes is mediated by p14 and required for signal transduction. Dev Cell 3: 803-14.

10. Nada S, Hondo A, Kasai A, Koike M, Saito K, Uchiyama Y *et al.* (2009) The novel lipid raft adaptor p18 controls endosome dynamics by anchoring the MEK-ERK pathway to late endosomes. EMBO J 28: 477-89.

11. Sancak Y, Bar-Peled L, Zoncu R, Markhard AL, Nada S Sabatini DM (2010) Ragulator-Rag complex targets mTORC1 to the lysosomal surface and is necessary for its activation by amino acids. Cell 141: 290-303.

12. Bar-Peled L, Schweitzer LD, Zoncu R Sabatini DM (2012) Ragulator is a GEF for the rag GTPases that signal amino acid levels to mTORC1. Cell 150: 1196-208.

13. Teis D, Taub N, Kurzbauer R, Hilber D, de Araujo ME, Erlacher M *et al.* (2006) p14-MP1-MEK1 signaling regulates endosomal traffic and cellular proliferation during tissue homeostasis. J Cell Biol 175: 861-8.

14. Yao Y, Wang J, Yoshida S, Nada S, Okada M Inoki K (2016) Role of Ragulator in the Regulation of Mechanistic Target of Rapamycin Signaling in Podocytes and Glomerular Function. J Am Soc Nephrol 27: 3653-3665.

15. Zoncu R, Bar-Peled L, Efeyan A, Wang S, Sancak Y Sabatini DM (2011) mTORC1 senses lysosomal amino acids through an inside-out mechanism that requires the vacuolar H(+)-ATPase. Science 334: 678-83.

16. Howell JJ Manning BD (2011) mTOR couples cellular nutrient sensing to organismal metabolic homeostasis. Trends Endocrinol Metab 22: 94-102.

17. Kholodenko BN Birtwistle MR (2009) Four-dimensional dynamics of MAPK information processing systems. Wiley Interdiscip Rev Syst Biol Med 1: 28-44.

18. Kolch W (2005) Coordinating ERK/MAPK signalling through scaffolds and inhibitors. Nat Rev Mol Cell Biol 6: 827-37.

19. Ma XM Blenis J (2009) Molecular mechanisms of mTOR-mediated translational control. Nat Rev Mol Cell Biol 10: 307-18.

20. Scheffler JM, Sparber F, Tripp CH, Herrmann C, Humenberger A, Blitz J *et al.* (2014) LAMTOR2 regulates dendritic cell homeostasis through FLT3-dependent mTOR signalling. Nat Commun 5: 5138.

21. Sparber F, Tripp CH, Komenda K, Scheffler JM, Clausen BE, Huber LA *et al.* (2015) The late endosomal adaptor molecule p14 (LAMTOR2) regulates TGFbeta1-mediated homeostasis of Langerhans cells. J Invest Dermatol 135: 119-129.

22. Sparber F, Scheffler JM, Amberg N, Tripp CH, Heib V, Hermann M *et al.* (2014) The late endosomal adaptor molecule p14 (LAMTOR2) represents a novel regulator of Langerhans cell homeostasis. Blood 123: 217-27.

23. Łyszkiewicz M, Kotlarz D, Ziętara N, Brandes G, Diestelhorst J, Glage S *et al.* (2019) LAMTOR2 (p14) Controls B Cell Differentiation by Orchestrating Endosomal BCR Trafficking. Frontiers in immunology 10: 497-497.

24. Notarangelo LD (2010) Primary immunodeficiencies. J Allergy Clin Immunol 125: S182-94.

25. Fischer A (2004) Human primary immunodeficiency diseases: a perspective. Nat Immunol 5: 23-30.

26. Modell V, Orange JS, Quinn J Modell F (2018) Global report on primary immunodeficiencies: 2018 update from the Jeffrey Modell Centers

Network on disease classification, regional trends, treatment modalities, and physician reported outcomes. Immunol Res 66: 367-380.

27. Tangye SG, Al-Herz W, Bousfiha A, Cunningham-Rundles C, Franco JL, Holland SM *et al.* (2022) Human Inborn Errors of Immunity: 2022 Update on the Classification from the International Union of Immunological Societies Expert Committee. J Clin Immunol 1-35.

28. Tangye SG, Al-Herz W, Bousfiha A, Chatila T, Cunningham-Rundles C, Etzioni A *et al.* (2020) Human Inborn Errors of Immunity: 2019 Update on the Classification from the International Union of Immunological Societies Expert Committee. J Clin Immunol 40: 24-64.

29. Heimall JR, Hagin D, Hajjar J, Henrickson SE, Hernandez-Trujillo HS, Tan Y *et al.* (2018) Use of Genetic Testing for Primary Immunodeficiency Patients. J Clin Immunol 38: 320-329.

30. Bohn G, Allroth A, Brandes G, Thiel J, Glocker E, Schaffer AA *et al.* (2007) A novel human primary immunodeficiency syndrome caused by deficiency of the endosomal adaptor protein p14. Nat Med 13: 38-45.

31. Langemeier J, Schrom EM, Rabner A, Radtke M, Zychlinski D, Saborowski A *et al.* (2012) A complex immunodeficiency is based on U1 snRNP-mediated poly(A) site suppression. Embo j 31: 4035-44.

32. Dell'Angelica EC (2007) Bad signals jam organelle traffic. Nature Medicine 13: 31-32.

33. Jung J, Bohn G, Allroth A, Boztug K, Brandes G, Sandrock I *et al.* (2006) Identification of a homozygous deletion in the AP3B1 gene causing Hermansky-Pudlak syndrome, type 2. Blood 108: 362-369.

34. Feng L, Seymour AB, Jiang S, To A, Peden AA, Novak EK *et al.* (1999) The β3A Subunit Gene (Ap3B1) of the Ap-3 Adaptor Complex Is Altered in the Mouse Hypopigmentation Mutant Pearl, a Model for Hermansky-Pudlak Syndrome and Night Blindness. Human Molecular Genetics 8: 323-330.

35. Ammann S, Schulz A, Krägeloh-Mann I, Dieckmann NMG, Niethammer K, Fuchs S *et al.* (2016) Mutations in AP3D1 associated with immunodeficiency and seizures define a new type of Hermansky-Pudlak syndrome. Blood 127: 997-1006.

36. Elewaut D, Lawton AP, Nagarajan NA, Maverakis E, Khurana A, Honing S *et al.* (2003) The adaptor protein AP-3 is required for CD1d-mediated antigen presentation of glycosphingolipids and development of Valpha14i NKT cells. The Journal of experimental medicine 198: 1133-1146.

37. Van Kaer L, Parekh VV Wu L (2011) Invariant natural killer T cells: bridging innate and adaptive immunity. Cell Tissue Res 343: 43-55.

38. Wu L Van Kaer L (2011) Natural killer T cells in health and disease. Frontiers in bioscience (Scholar edition) 3: 236-251.

39. Egawa T, Eberl G, Taniuchi I, Benlagha K, Geissmann F, Hennighausen L *et al.* (2005) Genetic evidence supporting selection of the Valpha14i NKT cell lineage from double-positive thymocyte precursors. Immunity 22: 705-16.

40. Montoya CJ, Pollard D, Martinson J, Kumari K, Wasserfall C, Mulder CB *et al.* (2007) Characterization of human invariant natural killer T subsets in health and disease using a novel invariant natural killer T cell-clonotypic monoclonal antibody, 6B11. Immunology 122: 1-14.

41. Germain RN (2002) T-cell development and the CD4–CD8 lineage decision. Nature Reviews Immunology 2: 309-322.

42. Chan S, Correia-Neves M, Dierich A, Benoist C Mathis D (1998) Visualization of CD4/CD8 T cell commitment. The Journal of experimental medicine 188: 2321-2333.

43. Bezbradica JS, Hill T, Stanic AK, Van Kaer L Joyce S (2005) Commitment toward the natural T (iNKT) cell lineage occurs at the

CD4+8+ stage of thymic ontogeny. Proceedings of the National Academy of Sciences of the United States of America 102: 5114-5119.

44. Shissler SC Webb TJ (2019) The ins and outs of type I iNKT cell development. Mol Immunol 105: 116-130.

45. White AJ, Lucas B, Jenkinson WE Anderson G (2018) Invariant NKT Cells and Control of the Thymus Medulla. The Journal of Immunology 200: 3333-3339.

46. Chan A, Berzins S Godfrey D (2010) Transcriptional regulation of lymphocyte development. Developing NKT cells need their (E) protein. Immunology and cell biology 88: 507-9.

47. Krangel MS (2009) Mechanics of T cell receptor gene rearrangement. Current opinion in immunology 21: 133-139.

48. Birkholz AM Kronenberg M (2015) Antigen specificity of invariant natural killer T-cells. Biomedical Journal 38: 470-483.

49. Brigl M Brenner MB (2004) CD1: Antigen Presentation and T Cell Function. Annual Review of Immunology 22: 817-890.

50. Liu Y, Goff RD, Zhou D, Mattner J, Sullivan BA, Khurana A *et al.* (2006) A modified alpha-galactosyl ceramide for staining and stimulating natural killer T cells. J Immunol Methods 312: 34-9.

51. D'Cruz LM, Knell J, Fujimoto JK Goldrath AW (2010) An essential role for the transcription factor HEB in thymocyte survival, Tcra rearrangement and the development of natural killer T cells. Nat Immunol 11: 240-9.

52. Sharma A, Berga-Bolanos R Sen JM (2014) T cell factor-1 controls the lifetime of CD4+ CD8+ thymocytes in vivo and distal T cell receptor alpha-chain rearrangement required for NKT cell development. PLoS One 9: e115803.

53. Hu T, Simmons A, Yuan J, Bender TP Alberola-Ila J (2010) The transcription factor c-Myb primes CD4+CD8+ immature thymocytes for selection into the iNKT lineage. Nat Immunol 11: 435-41.

54. Van Kaer L (2005) alpha-Galactosylceramide therapy for autoimmune diseases: prospects and obstacles. Nat Rev Immunol 5: 31-42.

55. Sprent J Surh C (2011) Normal T cell homeostasis: The conversion of naive cells into memory-phenotype cells. Nature immunology 12: 478-84.

56. Zimmer MI, Colmone A, Felio K, Xu H, Ma A Wang CR (2006) A cell-type specific CD1d expression program modulates invariant NKT cell development and function. J Immunol 176: 1421-30.

57. Sillé FC, Boxem M, Sprengers D, Veerapen N, Besra G Boes M (2009) Distinct requirements for CD1d intracellular transport for development of V(alpha)14 iNKT cells. J Immunol 183: 1780-8.

58. Vartabedian VF, Savage PB Teyton L (2016) The processing and presentation of lipids and glycolipids to the immune system. Immunological reviews 272: 109-119.

59. Chiu Y-H, Park S-H, Benlagha K, Forestier C, Jayawardena-Wolf J, Savage PB *et al.* (2002) Multiple defects in antigen presentation and T cell development by mice expressing cytoplasmic tail–truncated CD1d. Nature Immunology 3: 55-60.

60. Coles MC Raulet DH (2000) NK1.1+ T cells in the liver arise in the thymus and are selected by interactions with class I molecules on CD4+CD8+ cells. J Immunol 164: 2412-8.

61. Rodionov DG Bakke O (1998) Medium chains of adaptor complexes AP-1 and AP-2 recognize leucine-based sorting signals from the invariant chain. J Biol Chem 273: 6005-8.

62. Das R, Sant'Angelo DB Nichols KE (2010) Transcriptional control of invariant NKT cell development. Immunological reviews 238: 195-215.

63. Jordan MS, Smith JE, Burns JC, Austin J-ET, Nichols KE, Aschenbrenner AC *et al.* (2008) Complementation in trans of altered thymocyte development in mice expressing mutant forms of the adaptor molecule SLP76. Immunity 28: 359-369.

64. Arase H, Ono S, Arase N, Park SY, Wakizaka K, Watanabe H *et al.* (1995) Developmental arrest of NK1.1+ T cell antigen receptor (TCR)-alpha/beta+ T cells and expansion of NK1.1+ TCR-gamma/delta+ T cell development in CD3 zeta-deficient mice. The Journal of experimental medicine 182: 891-895.

65. Gadue P, Morton N Stein PL (1999) The Src family tyrosine kinase Fyn regulates natural killer T cell development. The Journal of experimental medicine 190: 1189-1196.

66. Zhang W, Sommers CL, Burshtyn DN, Stebbins CC, DeJarnette JB, Trible RP *et al.* (1999) Essential role of LAT in T cell development. Immunity 10: 323-32.

67. Chan G, Hanke T Fischer KD (2001) Vav-1 regulates NK T cell development and NK cell cytotoxicity. Eur J Immunol 31: 2403-10.

68. Iwabuchi K, Iwabuchi C, Tone S, Itoh D, Tosa N, Negishi I *et al.* (2001) Defective development of NK1.1+ T-cell antigen receptor alphabeta+ cells in zeta-associated protein 70 null mice with an accumulation of NK1.1+ CD3- NK-like cells in the thymus. Blood 97: 1765-75.

69. Felices M Berg LJ (2008) The Tec kinases Itk and Rlk regulate NKT cell maturation, cytokine production, and survival. J Immunol 180: 3007-18.

70. Griewank K, Borowski C, Rietdijk S, Wang N, Julien A, Wei DG *et al.* (2007) Homotypic interactions mediated by Slamf1 and Slamf6 receptors control NKT cell lineage development. Immunity 27: 751-62.

71. Borowski C Bendelac A (2005) Signaling for NKT cell development: the SAP-FynT connection. The Journal of experimental medicine 201: 833-836.

72. Godfrey DI, Stankovic S Baxter AG (2010) Raising the NKT cell family. Nature Immunology 11: 197-206.

73. Lee YJ, Holzapfel KL, Zhu J, Jameson SC Hogquist KA (2013) Steady-state production of IL-4 modulates immunity in mouse strains and is determined by lineage diversity of iNKT cells. Nat Immunol 14: 1146-54.

74. Cameron G Godfrey DI (2018) Differential surface phenotype and context-dependent reactivity of functionally diverse NKT cells. Immunol Cell Biol

75. Wang YX. *Natural killer T (NKT) lymphocytes regulate of intestinal tumor immunity*. 2017.

76. Gorentla BK Zhong X-P (2012) T cell Receptor Signal Transduction in T lymphocytes. Journal of clinical & cellular immunology 2012: 5-5.

77. Krishna S Zhong X (2013) Role of diacylglycerol kinases in T cell development and function. Critical reviews in immunology 33: 97-118.

78. Yang W, Gorentla B, Zhong X-P Shin J (2015) mTOR and its tight regulation for iNKT cell development and effector function. Molecular immunology 68: 536-545.

79. Hu T, Gimferrer I, Simmons A, Wiest D Alberola-Ila J (2011) The Ras/MAPK pathway is required for generation of iNKT cells. PloS one 6: e19890-e19890.

80. Inoki K, Li Y, Zhu T, Wu J Guan KL (2002) TSC2 is phosphorylated and inhibited by Akt and suppresses mTOR signalling. Nat Cell Biol 4: 648-57.

81. Zhang L, Tschumi BO, Corgnac S, Rüegg MA, Hall MN, Mach J-P *et al.* (2014) Mammalian Target of Rapamycin Complex 1 Orchestrates Invariant NKT Cell Differentiation and Effector Function. The Journal of Immunology 193: 1759.

82. Stanic AK, Bezbradica JS, Park JJ, Van Kaer L, Boothby MR Joyce S (2004) Cutting edge: the ontogeny and function of Va14Ja18 natural T lymphocytes require signal processing by protein kinase C theta and NF-kappa B. J Immunol 172: 4667-71.

83. Schmidt-Supprian M, Tian J, Grant EP, Pasparakis M, Maehr R, Ovaa H *et al.* (2004) Differential dependence of CD4+CD25+ regulatory and natural killer-like T cells on signals leading to NF-kappaB activation. Proceedings of the National Academy of Sciences of the United States of America 101: 4566-4571.

84. Sivakumar V, Hammond KJ, Howells N, Pfeffer K Weih F (2003) Differential requirement for Rel/nuclear factor kappa B family members in natural killer T cell development. J Exp Med 197: 1613-21.

85. Dose M, Sleckman BP, Han J, Bredemeyer AL, Bendelac A Gounari F (2009) Intrathymic proliferation wave essential for Vα14⁺ natural killer T cell development depends on c-Myc. Proceedings of the National Academy of Sciences 106: 8641-8646.

86. Godfrey DI, Stankovic S Baxter AG (2009) Developing NKT cells need their calcium. Nature Immunology 10: 231-233.

87. Dutta M, Kraus ZJ, Gomez-Rodriguez J, Hwang SH, Cannons JL, Cheng J *et al.* (2013) A role for Ly108 in the induction of promyelocytic zinc finger transcription factor in developing thymocytes. J Immunol 190: 2121-8.

88. Bassiri H Nichols K (2009) It's up to you Egr2. Immunology and cell biology 87: 361-3.

89. Lazarevic V, Zullo AJ, Schweitzer MN, Staton TL, Gallo EM, Crabtree GR *et al.* (2009) The gene encoding early growth response 2, a target of the transcription factor NFAT, is required for the development and maturation of natural killer T cells. Nature immunology 10: 306-313.

90. Townsend MJ, Weinmann AS, Matsuda JL, Salomon R, Farnham PJ, Biron CA *et al.* (2004) T-bet regulates the terminal maturation and homeostasis of NK and Valpha14i NKT cells. Immunity 20: 477-94.

91. Latour S, Gish G, Helgason CD, Humphries RK, Pawson T Veillette A (2001) Regulation of SLAM-mediated signal transduction by SAP, the X-linked lymphoproliferative gene product. Nat Immunol 2: 681-90.

92. Cannons JL, Yu LJ, Hill B, Mijares LA, Dombroski D, Nichols KE *et al.* (2004) SAP regulates T(H)2 differentiation and PKC-theta-mediated activation of NF-kappaB1. Immunity 21: 693-706.

93. Bernin H, Fehling H, Marggraff C, Tannich E Lotter H (2016) The cytokine profile of human NKT cells and PBMCs is dependent on donor sex and stimulus. Medical microbiology and immunology 205: 321-332.

94. Bendelac A, Rivera MN, Park S-H Roark JH (1997) MOUSE CD1-SPECIFIC NK1 T CELLS: Development, Specificity, and Function. Annual Review of Immunology 15: 535-562.

95. Hung LC, Lin CC, Hung SK, Wu BC, Jan MD, Liou SH *et al.* (2007) A synthetic analog of alpha-galactosylceramide induces macrophage activation via the TLR4-signaling pathways. Biochem Pharmacol 73: 1957-70.

96. Brigl M, Bry L, Kent SC, Gumperz JE Brenner MB (2003) Mechanism of CD1d-restricted natural killer T cell activation during microbial infection. Nat Immunol 4: 1230-7.

97. Kumar H, Belperron A, Barthold SW Bockenstedt LK (2000) Cutting edge: CD1d deficiency impairs murine host defense against the spirochete, Borrelia burgdorferi. J Immunol 165: 4797-801.

98. Exley MA, Bigley NJ, Cheng O, Shaulov A, Tahir SM, Carter QL *et al.* (2003) Innate immune response to encephalomyocarditis virus infection mediated by CD1d. Immunology 110: 519-26.

99. Mattner J, Debord KL, Ismail N, Goff RD, Cantu C, 3rd, Zhou D *et al.* (2005) Exogenous and endogenous glycolipid antigens activate NKT cells during microbial infections. Nature 434: 525-9.

100. Joyee AG, Qiu H, Wang S, Fan Y, Bilenki L Yang X (2007) Distinct NKT cell subsets are induced by different Chlamydia species leading to differential adaptive immunity and host resistance to the infections. J Immunol 178: 1048-58.

101. Grubor-Bauk B, Simmons A, Mayrhofer G Speck PG (2003) Impaired clearance of herpes simplex virus type 1 from mice lacking CD1d or NKT cells expressing the semivariant V alpha 14-J alpha 281 TCR. J Immunol 170: 1430-4.

102. Ashkar AA Rosenthal KL (2003) Interleukin-15 and natural killer and NKT cells play a critical role in innate protection against genital herpes simplex virus type 2 infection. J Virol 77: 10168-71.

103. Xu X, Pocock GM, Sharma A, Peery SL, Fites JS, Felley L *et al.* (2016) Human iNKT Cells Promote Protective Inflammation by Inducing Oscillating Purinergic Signaling in Monocyte-Derived DCs. Cell Rep 16: 3273-3285.

104. Vasan S, Poles MA, Horowitz A, Siladji EE, Markowitz M Tsuji M (2007) Function of NKT cells, potential anti-HIV effector cells, are improved by beginning HAART during acute HIV-1 infection. Int Immunol 19: 943-51.

105. Inoue M, Kanto T, Miyatake H, Itose I, Miyazaki M, Yakushijin T *et al.* (2006) Enhanced ability of peripheral invariant natural killer T cells to produce IL-13 in chronic hepatitis C virus infection. J Hepatol 45: 190-6.

106. De Santo C, Salio M, Masri SH, Lee LY, Dong T, Speak AO *et al.* (2008) Invariant NKT cells reduce the immunosuppressive activity of influenza A virus-induced myeloid-derived suppressor cells in mice and humans. J Clin Invest 118: 4036-48.

107. Beitzen-Heineke A, Bouzani M, Schmitt AL, Kurzai O, Hünniger K, Einsele H *et al.* (2016) Human Invariant Natural Killer T cells possess immune-modulating functions during Aspergillus infection. Med Mycol 54: 169-76.

108. Terabe M Berzofsky JA (2008) The role of NKT cells in tumor immunity. Advances in cancer research 101: 277-348.

109. Smyth MJ, Thia KY, Street SE, Cretney E, Trapani JA, Taniguchi M *et al.* (2000) Differential tumor surveillance by natural killer (NK) and NKT cells. J Exp Med 191: 661-8.

110. Kobayashi E, Motoki K, Uchida T, Fukushima H Koezuka Y (1995) KRN7000, a novel immunomodulator, and its antitumor activities. Oncol Res 7: 529-34.

111. Motoki K, Morita M, Kobayashi E, Uchida T, Akimoto K, Fukushima H *et al.* (1995) Immunostimulatory and antitumor activities of monoglycosylceramides having various sugar moieties. Biol Pharm Bull 18: 1487-91.

112. Toura I, Kawano T, Akutsu Y, Nakayama T, Ochiai T Taniguchi M (1999) Cutting edge: inhibition of experimental tumor metastasis by dendritic cells pulsed with alpha-galactosylceramide. J Immunol 163: 2387-91.

113. Schmieg J, Yang G, Franck RW Tsuji M (2003) Superior protection against malaria and melanoma metastases by a C-glycoside analogue of the natural killer T cell ligand alpha-Galactosylceramide. J Exp Med 198: 1631-41.

114. Hayakawa Y, Rovero S, Forni G Smyth MJ (2003) Alpha-galactosylceramide (KRN7000) suppression of chemical- and oncogene-dependent carcinogenesis. Proc Natl Acad Sci U S A 100: 9464-9.

115. Cui J, Shin T, Kawano T, Sato H, Kondo E, Toura I *et al.* (1997) Requirement for Valpha14 NKT cells in IL-12-mediated rejection of tumors. Science 278: 1623-6.

116. Smyth MJ, Taniguchi M Street SE (2000) The anti-tumor activity of IL-12: mechanisms of innate immunity that are model and dose dependent. J Immunol 165: 2665-70.

117. Ishihara S, Nieda M, Kitayama J, Osada T, Yabe T, Kikuchi A *et al.* (2000) Alpha-glycosylceramides enhance the antitumor cytotoxicity of hepatic lymphocytes obtained from cancer patients by activating CD3-CD56+ NK cells in vitro. J Immunol 165: 1659-64.

118. Dhodapkar MV, Geller MD, Chang DH, Shimizu K, Fujii S, Dhodapkar KM *et al.* (2003) A reversible defect in natural killer T cell function characterizes the progression of premalignant to malignant multiple myeloma. J Exp Med 197: 1667-76.

119. Tahir SM, Cheng O, Shaulov A, Koezuka Y, Bubley GJ, Wilson SB *et al.* (2001) Loss of IFN-gamma production by invariant NK T cells in advanced cancer. J Immunol 167: 4046-50.

120. Tachibana T, Onodera H, Tsuruyama T, Mori A, Nagayama S, Hiai H *et al.* (2005) Increased intratumor Valpha24-positive natural killer T cells: a prognostic factor for primary colorectal carcinomas. Clin Cancer Res 11: 7322-7.

121. Motohashi S, Ishikawa A, Ishikawa E, Otsuji M, Iizasa T, Hanaoka H *et al.* (2006) A phase I study of in vitro expanded natural killer T cells in patients with advanced and recurrent non-small cell lung cancer. Clin Cancer Res 12: 6079-86.

122. Ishikawa A, Motohashi S, Ishikawa E, Fuchida H, Higashino K, Otsuji M *et al.* (2005) A phase I study of alpha-galactosylceramide (KRN7000)-pulsed dendritic cells in patients with advanced and recurrent non-small cell lung cancer. Clin Cancer Res 11: 1910-7.

123. Chang DH, Osman K, Connolly J, Kukreja A, Krasovsky J, Pack M *et al.* (2005) Sustained expansion of NKT cells and antigen-specific T cells after injection of alpha-galactosyl-ceramide loaded mature dendritic cells in cancer patients. J Exp Med 201: 1503-17.

124. Akbari O, Stock P, Meyer E, Kronenberg M, Sidobre S, Nakayama T *et al.* (2003) Essential role of NKT cells producing IL-4 and IL-13 in the development of allergen-induced airway hyperreactivity. Nat Med 9: 582-8.

125. Coppieters K, Dewint P, Van Beneden K, Jacques P, Seeuws S, Verbruggen G *et al.* (2007) NKT cells: manipulable managers of joint inflammation. Rheumatology 46: 565-571.

126. Tupin E, Nicoletti A, Elhage R, Rudling M, Ljunggren H-G, Hansson GK *et al.* (2004) CD1d-dependent activation of NKT cells aggravates atherosclerosis. The Journal of experimental medicine 199: 417-422.

127. Nakai Y, Iwabuchi K, Fujii S, Ishimori N, Dashtsoodol N, Watano K *et al.* (2004) Natural killer T cells accelerate atherogenesis in mice. Blood 104: 2051-9.

128. Campos RA, Szczepanik M, Itakura A, Akahira-Azuma M, Sidobre S, Kronenberg M *et al.* (2003) Cutaneous immunization rapidly activates liver invariant Valpha14 NKT cells stimulating B-1 B cells to initiate T cell recruitment for elicitation of contact sensitivity. The Journal of experimental medicine 198: 1785-1796.

129. Heller F, Fuss IJ, Nieuwenhuis EE, Blumberg RS Strober W (2002) Oxazolone colitis, a Th2 colitis model resembling ulcerative colitis, is mediated by IL-13-producing NK-T cells. Immunity 17: 629-38.

130. Lappas CM, Day Y-J, Marshall MA, Engelhard VH Linden J (2006) Adenosine A2A receptor activation reduces hepatic ischemia reperfusion injury by inhibiting CD1d-dependent NKT cell activation. The Journal of experimental medicine 203: 2639-2648.

131. Wallace KL, Marshall MA, Ramos SI, Lannigan JA, Field JJ, Strieter RM *et al.* (2009) NKT cells mediate pulmonary inflammation and dysfunction in murine sickle cell disease through production of IFN-gamma and CXCR3 chemokines. Blood 114: 667-676.

132. Antunes L, Duarte de Souza AP, de Araújo PD, Pinto LA, Jones MH, Stein RT *et al.* (2018) iNKT cells are increased in children with severe therapy-resistant asthma. Allergol Immunopathol (Madr) 46: 175-180.

133. Koh YI Shim JU (2010) Association between sputum natural killer T cells and eosinophilic airway inflammation in human asthma. Int Arch Allergy Immunol 153: 239-48.

134. Burrello C, Pellegrino G, Giuffrè MR, Lovati G, Magagna I, Bertocchi A *et al.* (2019) Mucosa-associated microbiota drives pathogenic functions in IBD-derived intestinal iNKT cells. 2:

135. Pillai AB, George TI, Dutt S, Teo P Strober S (2007) Host NKT cells can prevent graft-versus-host disease and permit graft antitumor activity after bone marrow transplantation. J Immunol 178: 6242-51.

136. Araki M, Kondo T, Gumperz JE, Brenner MB, Miyake S Yamamura T (2003) Th2 bias of CD4+ NKT cells derived from multiple sclerosis in remission. Int Immunol 15: 279-88.

137. Sharif S, Arreaza GA, Zucker P, Mi QS, Sondhi J, Naidenko OV *et al.* (2001) Activation of natural killer T cells by alpha-galactosylceramide treatment prevents the onset and recurrence of autoimmune Type 1 diabetes. Nat Med 7: 1057-62.

138. Naumov YN, Bahjat KS, Gausling R, Abraham R, Exley MA, Koezuka Y *et al.* (2001) Activation of CD1d-restricted T cells protects NOD mice

from developing diabetes by regulating dendritic cell subsets. Proceedings of the National Academy of Sciences of the United States of America 98: 13838-13843.

139. Chen J, Wu M, Wang J Li X (2015) Immunoregulation of NKT Cells in Systemic Lupus Erythematosus. J Immunol Res 2015: 206731.

140. Gabriel L, Morley BJ Rogers NJ (2009) The role of iNKT cells in the immunopathology of systemic lupus erythematosus. Ann N Y Acad Sci 1173: 435-41.

141. Wilson SB, Kent SC, Patton KT, Orban T, Jackson RA, Exley M *et al.* (1998) Extreme Th1 bias of invariant Valpha24JalphaQ T cells in type 1 diabetes. Nature 391: 177-81.

142. Démoulins T, Gachelin G, Bequet D Dormont D (2003) A biased Valpha24+ T-cell repertoire leads to circulating NKT-cell defects in a multiple sclerosis patient at the onset of his disease. Immunol Lett 90: 223-8.

143. van der Vliet HJ, von Blomberg BM, Nishi N, Reijm M, Voskuyl AE, van Bodegraven AA *et al.* (2001) Circulating V(alpha24+) Vbeta11+ NKT cell numbers are decreased in a wide variety of diseases that are characterized by autoreactive tissue damage. Clin Immunol 100: 144-8.

144. Park O, Jeong W-I, Wang L, Wang H, Lian Z-X, Gershwin ME *et al.* (2009) Diverse roles of invariant natural killer T cells in liver injury and fibrosis induced by carbon tetrachloride. Hepatology (Baltimore, Md.) 49: 1683-1694.

145. Kumar V (2013) NKT-cell subsets: Promoters and protectors in inflammatory liver disease. Journal of Hepatology 59: 618-620.

146. Notas G, Kisseleva T Brenner D (2009) NK and NKT cells in liver injury and fibrosis. Clin Immunol 130: 16-26.

147. de Lalla C, Galli G, Aldrighetti L, Romeo R, Mariani M, Monno A *et al.* (2004) Production of profibrotic cytokines by invariant NKT cells characterizes cirrhosis progression in chronic viral hepatitis. J Immunol 173: 1417-25.

148. Syn WK, Oo YH, Pereira TA, Karaca GF, Jung Y, Omenetti A *et al.* (2010) Accumulation of natural killer T cells in progressive nonalcoholic fatty liver disease. Hepatology 51: 1998-2007.

149. Harada K, Isse K, Tsuneyama K, Ohta H Nakanuma Y (2003) Accumulating CD57 + CD3 + natural killer T cells are related to intrahepatic bile duct lesions in primary biliary cirrhosis. Liver International 23: 94-100.

150. Choi H-J, Geng Y, Cho H, Li S, Giri PK, Felio K *et al.* (2011) Differential requirements for the Ets transcription factor Elf-1 in the development of NKT cells and NK cells. Blood 117: 1880-1887.

151. Nyambayar D, Iwabuchi K, Hedlund E, Murakawa S, Shirai K, Iwabuchi C *et al.* (2007) Characterization of NKT-cell hybridomas expressing invariant T-cell antigen receptors. J Clin Exp Hematop 47: 1-8.

152. Scholten D, Trebicka J, Liedtke C Weiskirchen R (2015) The carbon tetrachloride model in mice. Lab Anim 49: 4-11.

153. Gapin L, Matsuda JL, Surh CD Kronenberg M (2001) NKT cells derive from double-positive thymocytes that are positively selected by CD1d. Nat Immunol 2: 971-8.

154. Dinh XT, Stanley D, Smith LD, Moreau M, Berzins SP, Gemiarto A *et al.* (2021) Modulation of TCR signalling components occurs prior to positive selection and lineage commitment in iNKT cells. Scientific Reports 11: 23650.

155. Qiao Y, Zhu L, Sofi H, Lapinski PE, Horai R, Mueller K *et al.* (2012) Development of promyelocytic leukemia zinc finger-expressing innate CD4 T cells requires stronger T-cell receptor signals than conventional

CD4 T cells. Proceedings of the National Academy of Sciences 109: 16264.

156. Jayawardena-Wolf J Bendelac A (2001) CD1 and lipid antigens: intracellular pathways for antigen presentation. Current Opinion in Immunology 13: 109-113.

157. Shin J, Wang S, Deng W, Wu J, Gao J Zhong X-P (2014) Mechanistic target of rapamycin complex 1 is critical for invariant natural killer T-cell development and effector function. Proceedings of the National Academy of Sciences 111: E776-E783.

158. Ansari AR Liu H (2017) Acute Thymic Involution and Mechanisms for Recovery. Archivum Immunologiae et Therapiae Experimentalis 65: 401-420.

159. Jírová D, Sperlingová I, Halasková M, Bendová H Dabrowská L (1996) Immunotoxic effects of carbon tetrachloride--the effect on morphology and function of the immune system in mice. Cent Eur J Public Health 4: 16-20.

160. Wang SD, Huang KJ, Lin YS Lei HY (1994) Sepsis-induced apoptosis of the thymocytes in mice. The Journal of Immunology 152: 5014-5021.

161. Hick RW, Gruver AL, Ventevogel MS, Haynes BF Sempowski GD (2006) Leptin selectively augments thymopoiesis in leptin deficiency and lipopolysaccharide-induced thymic atrophy. Journal of immunology (Baltimore, Md. : 1950) 177: 169-176.

162. Uldrich AP, Crowe NY, Kyparissoudis K, Pellicci DG, Zhan Y, Lew AM *et al.* (2005) NKT cell stimulation with glycolipid antigen in vivo: costimulation-dependent expansion, Bim-dependent contraction, and hyporesponsiveness to further antigenic challenge. Journal of immunology (Baltimore, Md. : 1950) 175: 3092-3101.

163. Wilson MT, Johansson C, Olivares-Villagómez D, Singh AK, Stanic AK, Wang C-R *et al.* (2003) The response of natural killer T cells to glycolipid

antigens is characterized by surface receptor down-modulation and expansion. Proceedings of the National Academy of Sciences of the United States of America 100: 10913-10918.

164. Colaço A Jäättelä M (2017) Ragulator—a multifaceted regulator of lysosomal signaling and trafficking. Journal of Cell Biology 216: 3895-3898.

165. Yordanov TE, Hipolito VEB, Liebscher G, Vogel GF, Stasyk T, Herrmann C *et al.* (2019) Biogenesis of lysosome-related organelles complex-1 (BORC) regulates late endosomal/lysosomal size through PIKfyve-dependent phosphatidylinositol-3,5-bisphosphate. 20: 674-696.

166. Taub N, Nairz M, Hilber D, Hess MW, Weiss G Huber LA (2012) The late endosomal adaptor p14 is a macrophage host-defense factor against Salmonella infection. Journal of Cell Science 125: 2698.

167. Pellicci DG, Koay H-F Berzins SP (2020) Thymic development of unconventional T cells: how NKT cells, MAIT cells and γδ T cells emerge. Nature Reviews Immunology 20: 756-770.

168. Zarin P, Chen ELY, In TSH, Anderson MK Zúñiga-Pflücker JC (2015) Gamma delta T-cell differentiation and effector function programming, TCR signal strength, when and how much? Cellular Immunology 296: 70-75.

169. Gascoigne NR, Rybakin V, Acuto O Brzostek J (2016) TCR Signal Strength and T Cell Development. Annual review of cell and developmental biology 32: 327-348.

170. Moran AE, Holzapfel KL, Xing Y, Cunningham NR, Maltzman JS, Punt J *et al.* (2011) T cell receptor signal strength in Treg and iNKT cell development demonstrated by a novel fluorescent reporter mouse. J Exp Med 208: 1279-89.

171. Billard MJ, Gruver AL Sempowski GD (2011) Acute Endotoxin-Induced Thymic Atrophy Is Characterized By Intrathymic Inflammatory and Wound Healing Responses. PLOS ONE 6: e17940.